ELSEVIER

Contents lists available at ScienceDirect

### Journal of Computational Physics

www.elsevier.com/locate/jcp



## Positivity-preserving high order finite difference WENO schemes for compressible Navier-Stokes equations \*\*



Chuan Fan <sup>a</sup>, Xiangxiong Zhang <sup>b</sup>, Jianxian Qiu <sup>c,\*</sup>

- <sup>a</sup> School of Mathematical Sciences, Xiamen University, Xiamen, Fujian 361005, PR China
- <sup>b</sup> Department of Mathematics, Purdue University, West Lafayette, IN 47907-2067, USA
- <sup>c</sup> School of Mathematical Sciences and Fujian Provincial Key Laboratory of Mathematical Modeling and High-Performance Scientific Computing, Xiamen University, Xiamen, Fujian 361005, PR China

#### ARTICLE INFO

# Article history: Received 16 November 2021 Received in revised form 4 May 2022 Accepted 30 June 2022 Available online 22 July 2022

Keywords:
Positivity-preserving
Compressible Navier-Stokes equations
WENO
Finite difference
High order accuracy

#### ABSTRACT

In this paper, we construct a high order weighted essentially non-oscillatory (WENO) finite difference discretization for compressible Navier-Stokes (NS) equations, which is rendered positivity-preserving of density and internal energy by a positivity-preserving flux splitting and a scaling positivity-preserving limiter. The novelty of this paper is WENO reconstruction performed on variables from a positivity-preserving convection diffusion flux splitting, which is different from conventional WENO schemes solving compressible NS equations. The core advantages of our proposed method are robustness and efficiency, which especially are suitable for solving tough demanding problems of both compressible Euler and NS equation including low density and low pressure flow regime. Moreover, in terms of computational cost, it is more efficient and easier to implement and extend to multi-dimensional problems than the positivity-preserving high order discontinuous Galerkin schemes and finite volume WENO scheme for solving compressible NS equations on rectangle domain. Benchmark tests demonstrate that the proposed positivity-preserving WENO schemes are high order accuracy, efficient and robust without excessive artificial viscosity for demanding problems involving with low density, low pressure, and fine structure.

© 2022 Elsevier Inc. All rights reserved.

#### 1. Introduction

The compressible NS equations are the most popular continuum model equations in gas dynamics. The system without external forces in conservative form can be written as

$$\mathbf{U}_t + \nabla \cdot \mathbf{F}^a = \nabla \cdot \mathbf{F}^d. \tag{1.1}$$

where  $\mathbf{U} = (\rho, \rho \mathbf{u}, E)^T$  are the conservative variables,  $\rho$  is the density,  $\mathbf{u} = (u, v, w)$  denote the velocity, the total energy  $E = \rho e + \frac{1}{2}\rho \|\mathbf{u}\|^2$  with e denoting the internal energy. The fluxes are the advection flux  $\mathbf{F}^a = (\rho \mathbf{u}, \rho \mathbf{u} \otimes \mathbf{u} + p \mathbb{I}, (E+p)\mathbf{U})^T$  and the diffusion flux  $\mathbf{F}^d = (0, \tau, \mathbf{u} \cdot \tau - \mathbf{q})^T$ , in which p is the pressure and  $\mathbb{I}$  is the unit tensor,  $\tau$  is the stress tensor and

E-mail addresses: fanchuan@stu.xmu.edu.cn (C. Fan), zhan1966@purdue.edu (X. Zhang), jxqiu@xmu.edu.cn (J. Qiu).

<sup>🌣</sup> C. Fan and J. Qiu were supported by NSFC grant 12071392. X. Zhang was supported by the NSF grant DMS-1913120.

<sup>\*</sup> Corresponding author.

**q** is the heat flux. The relations between conserved variables **U** and pressure p are given by equations of state (EOS). For a calorically ideal gas one has  $p = (\gamma - 1)\rho e$  where  $\gamma = 1.4$  can be taken for air.

The positivity of density  $\rho$  and pressure p (or internal energy e) is often desired for numerical schemes solving compressible Euler and NS equations. Of course it is needed for numerical solutions to be physical meaningful. More importantly, it is crucial to preserve positivity for the sake of nonlinear stability. In practice, emergence of negative density or pressure often results in blow-ups of computation. With negative density or pressure, the linearized compressible Euler equations are no longer hyperbolic, thus the initial value problem of linearized system is already ill-posed. A conservative positivity-preserving Eulerian scheme on fixed meshes is  $L^1$  stable for  $\rho$  and E, thus quite robust [28].

For the sake of robustness of schemes, we are interested in conservative schemes preserving the positivity. Define the internal energy function  $\rho e(\mathbf{U}) = E - \frac{1}{2}\rho \|\mathbf{u}\|^2$  and the set of admissible states as

$$G = \left\{ \mathbf{U} = \begin{pmatrix} \rho \\ \rho \mathbf{u} \\ E \end{pmatrix} : \rho > 0, \quad \rho e(\mathbf{U}) > 0 \right\}.$$
(1.2)

We only consider an EOS satisfying  $p > 0 \Leftrightarrow e > 0$ , e.g., the ideal gas EOS, so positivity of e is equivalent to positivity of p. For other equations of state such as Jones-Wilkins-Lee EOS [6], (1.2) on longer ensures positive pressure. Nonetheless, it suffices to preserve positivity of  $\rho$  and e for the sake of robustness. Moreover, G in (1.2) is always a convex set for any EOS since  $\rho e(\mathbf{U})$  is a concave function for  $\rho > 0$  and satisfies the Jensen's inequality  $\forall \mathbf{U}_1, \mathbf{U}_2 \in G$ ,  $\forall \lambda_1, \lambda_2 \geq 0, \lambda_1 + \lambda_2 = 1$ ,

$$\rho e(\lambda_1 \mathbf{U}_1 + \lambda_2 \mathbf{U}_2) \ge \lambda_1 \rho e(\mathbf{U}_1) + \lambda_2 \rho e(\mathbf{U}_2). \tag{1.3}$$

#### 1.1. WENO schemes for gas dynamics

Weighted essentially non-oscillatory (WENO) method [18] is a very successful high order accurate reconstruction method. The finite difference WENO scheme by Jiang and Shu in [15], which will be referred as WENO-JS scheme, and its variants are among the most popular high order schemes for hyperbolic problems such as gas dynamics applications [25]. In practice, the WENO-JS scheme provides stable numerical solutions for most problems of compressible Euler equations. On the other hand, for demanding problems involving extremely low density and pressure such as simulating astrophysical jets, the WENO method and the WENO-JS scheme may not be robust enough [25].

For stabilizing high order accurate schemes for demanding problems, a systematic method of designing bound-preserving or positivity-preserving limiters based on intrinsic properties in high order finite volume and discontinuous Galerkin (DG) methods were developed by Zhang and Shu in [30–33,35]. The Zhang-Shu method can be easily applied to finite volume WENO schemes. For the finite difference WENO scheme, the Zhang-Shu method can be extended through a special implementation for compressible Euler equations [34].

For rendering the finite difference WENO scheme positivity-preserving for compressible Euler equations, there are many other methods, e.g., [11,14,22,27]. All these methods are heavily dependent on first-order positivity-preserving schemes for compressible Euler equations, including the exact Godunov scheme, flux vector splitting scheme [9], Lax-Friedrichs schemes [21,31], HLLE schemes [2,4] and gas-kinetic schemes [26]. It is not straightforward at all to generalize these methods to compressible NS equations, since there are no standard low order positivity-preserving schemes for the NS diffusion operator, which is the key difficulty for designing positivity-preserving schemes for compressible NS equations.

For approximating diffusion operators, the robustness of WENO methods can be much improved by avoiding negative linear weights in reconstruction [19,20,24]. However, these WENO methods are still not robust for demanding gas dynamics tests, e.g., the positivity of density and pressure is not preserved. Without any positivity treatment, WENO schemes might not be stable for the low density and low pressure problems such as high Mach number astrophysical jets. Thus, it is necessary to enforce positivity in WENO schemes for the sake of robustness.

#### 1.2. Objective and related work

The objective in this paper is to design a conservative positivity-preserving high order accurate scheme for solving (1.1) in the finite difference framework. The Zhang-Shu method [31] can be generalized to positivity-preserving discontinuous Galerkin schemes solving the compressible NS equations [28], in which the key ingredient is a positivity-preserving nonlinear diffusion flux. Such a flux can also be used for constructing high order positivity-preserving finite volume methods [5]. The positivity-preserving techniques in Zhang-Shu method for DG and finite volume schemes [5,28,31] do not affect provable high order accuracy for smooth solutions satisfying  $\rho e \ge C > 0$  where C is a constant. The extension of the same techniques to the finite difference WENO scheme for Euler equations in [34] can maintain provable high order accuracy in the WENO scheme for smooth solutions with one additional assumption  $\rho e \ge C > 0$ . In this paper, we construct a high order accurate positivity-preserving finite difference WENO scheme for compressible NS equations by applying the same positivity-preserving nonlinear diffusion flux in the WENO implementation.

We emphasize that it is quite straightforward to construct a positivity-preserving finite difference scheme for NS equations in one dimension, see the appendix in [28]. The main difficulty of designing positivity-preserving finite difference

schemes lies in the multiple dimensional stress tensor. In this paper, the positivity of one-dimensional scheme can be easily extended to two dimensions due its construction.

There are also other positivity-preserving methods for compressible NS equations [8,10], but extensions of these methods to high order finite difference schemes seem difficult. A non-conventional WENO finite volume method can preserve bounds for scalar convection diffusion [29] but it is still nontrivial to generalize it to compressible NS equations.

#### 1.3. Contributions and organization of the paper

In this paper, we construct positivity-preserving high order finite difference WENO schemes for solving compressible NS equations. The key step is to reconstruct variables from a positivity-preserving convection diffusion flux splitting, which is different from conventional WENO schemes for diffusion terms. Compared to the positivity-preserving high order accurate DG schemes in [28] and finite volume WENO schemes in [5] for solving compressible NS equations, the positivity-preserving finite difference WENO schemes are more efficient and easier to implement, thanks to smaller memory cost compared to DG schemes, and lower computational cost than DG and finite volume schemes, especially for multi-dimensional problems.

The work of this paper is an extension of the positivity-preserving finite difference WENO scheme for compressible Euler equations in [34] to the compressible NS equations. When the Navier-Stokes equations reduce to Euler equations, i.e.,  $\mathbf{F}^d \equiv 0$ , the scheme in this paper will reduce to exactly the same scheme in [34]. However, the positivity-preserving diffusion flux splitting used in this paper is a nonlinear flux and its analytical properties such as artificial viscosity are not as well understood as the classical Lax-Friedrichs flux splitting used for compressible Euler equations in [34]. On the other hand, unlike the linear DG methods, the WENO reconstruction is a nonlinear operator thus using a nonlinear flux splitting seems more suitable in WENO schemes. Moreover, numerical tests on the classical WENO-JS schemes and a less diffusive scheme WENO-ZQ [36] suggest that the nonlinear diffusion positivity-preserving flux splitting can improve robustness significantly without inducing excessive artificial viscosity.

The organization of the paper is as follows. In Section 2, we review the basic idea of the finite difference WENO scheme and review the positivity-preserving high order finite volume scheme for compressible NS equations. In Section 3, we construct the positivity-preserving high order finite difference WENO schemes for compressible NS equations. A similar alternative positivity-preserving high order finite difference WENO scheme is discussed in Section 4. In Section 5, we consider a few benchmark tests for validating the performance. Concluding remarks are given in Section 6.

#### 2. Preliminaries

In this section, we first review the high order finite difference WENO scheme for scalar conservation laws [15], which can be regarded as a formal finite volume scheme for an auxiliary function. Then we review the high order positivity-preserving finite volume scheme for compressible NS equations [28]. These methods will be used for constructing a positivity-preserving finite difference scheme in Section 3.

#### 2.1. Review of the finite difference WENO scheme for scalar conservation laws

Consider the one-dimension scalar hyperbolic conservation law

$$u_t + f(u)_x = 0.$$
 (2.1)

Given a uniform grid  $x_i$  with spacing  $\Delta x_i$ , we define cells  $I_i = [x_{i-\frac{1}{2}}, x_{i+\frac{1}{2}}]$  where  $x_{i\pm\frac{1}{2}} = x_i \pm \frac{1}{2} \Delta x$ . Let  $u_i(t)$  be the numerical approximation to the exact solution u(x,t) at  $x_i$ . A conservative semi-discrete scheme for (2.1) is given by

$$\frac{du_i(t)}{dt} = -\frac{1}{\Delta x}(\hat{f}_{i+\frac{1}{2}} - \hat{f}_{i-\frac{1}{2}}),\tag{2.2}$$

where  $\hat{f}_{i+\frac{1}{2}}$  is the numerical flux, but not as a high order approximation of the flux f(u) at  $x_{i+\frac{1}{2}}$ . Assume there exists an auxiliary function h(x,t) satisfying

$$f(u(x,t)) = \frac{1}{\Delta x} \int_{x-\Delta x/2}^{x+\Delta x/2} h(\eta,t) d\eta, \quad \forall x.$$
 (2.3)

By (2.3),  $f(u(x_i, t))$  is the cell average of h(x, t) and

$$f(u(x_i,t))_x = \frac{1}{\Lambda x} [h(x_{i+\frac{1}{2}},t) - h(x_{i-\frac{1}{2}},t)]. \tag{2.4}$$

Thus if the numerical flux  $\hat{f}_{i+\frac{1}{2}}$  is a (2r+1)th order approximation to  $h_{i+\frac{1}{2}}=h(x_{i+\frac{1}{2}})$ , then  $\frac{1}{\Delta x}(\hat{f}_{i+\frac{1}{2}}-\hat{f}_{i-\frac{1}{2}})$  is a (2r+1)th order approximation to  $f(u(x_i))_x$ , which is the point of view for the high order conservative finite difference scheme in [15].

For linear equation f(u) = u, let  $\bar{h}_i(t) = \frac{1}{\Delta x} \int_{x_i - \Delta x/2}^{x_i + \Delta x/2} h(\eta, t) d\eta = u(x_i)$ , then by the interpretation above, the finite difference scheme (2.2) is also a formal finite volume scheme for the function h(x, t):

$$\frac{d\bar{h}_i(t)}{dt} = -\frac{1}{\Delta x}(\hat{h}_{i+\frac{1}{2}}^- - \hat{h}_{i-\frac{1}{2}}^-).$$

For the nonlinear scalar equation, with the consideration of stability, the upwind biasing is usually used by splitting the flux f(u) into two parts:  $f(u) = f^+(u) + f^-(u)$  with  $\frac{\mathrm{d} f^+(u)}{\mathrm{d} u} \geq 0$  and  $\frac{\mathrm{d} f^-(u)}{\mathrm{d} u} \leq 0$ . A simple Lax-Friedrichs splitting is applied as  $f^\pm(u) = \frac{1}{2}(f(u) \pm \alpha u)$  with  $\alpha = \max_u |f'(u)|$ , where the maximum can be taken globally or locally in the stencil of the WENO scheme. Assume there exist two functions  $h_\pm(x)$  depending on the mesh size  $\Delta x$ , such that

$$\frac{1}{2}\left(u\pm\frac{f(u)}{\alpha}\right) := z^{\pm}(u(x)) = \frac{1}{\Delta x} \int_{x-\Delta x/2}^{x+\Delta x/2} h_{\pm}(\eta) d\eta. \tag{2.5}$$

For convenience, we introduce the operator  $R_{\Delta x}$  as

$$h_{+} = R_{\Delta x}(z^{+}), h_{-} = R_{\Delta x}(z^{-}) \text{ or } z^{+} = R_{\Delta x}^{-1}(h_{+}), z^{-} = R_{\Delta x}^{-1}(h_{-}).$$

Notice that the flux  $f = \alpha(z^+ - z^-)$  and  $z^\pm$  satisfy  $\frac{dz^+}{du} \ge 0$  and  $\frac{dz^-}{du} \ge 0$ , thus it is equivalent to  $f^\pm$  by  $z^+ = \alpha f^+$  and  $z^- = -\alpha f^-$ .

Given cell averages of  $h_{\pm}(x)$ , i.e., point values  $z^{\pm}(u(x_i)) = \frac{1}{2}\left(u_i \pm \frac{f(u_i)}{\alpha}\right)$ , one can use the WENO reconstruction to obtain high order approximation to  $h_{\pm}(x_{i\pm\frac{1}{2}})$ , which are denoted as  $\hat{z}^{\pm}_{i\pm\frac{1}{2}}$ . Finally, the numerical flux is computed as  $\hat{f}_{i\pm\frac{1}{2}} = \alpha(\hat{z}^+_{i\pm\frac{1}{2}} - \hat{z}^-_{i\pm\frac{1}{2}})$ .

#### 2.2. A positivity-preserving high order finite volume scheme

The dimensionless compressible Navier-Stokes equations for ideal gas in one dimension are

$$\mathbf{U}_t + \mathbf{F}^a(\mathbf{U})_x = \mathbf{F}^d(\mathbf{U}, \mathbf{S})_x \tag{2.6}$$

with the flux function  $\mathbf{F}(\mathbf{U}, \mathbf{S}) = \mathbf{F}^{a}(\mathbf{U}) - \mathbf{F}^{d}(\mathbf{U}, \mathbf{S})$  and

$$\mathbf{S} = \mathbf{U}_{\mathsf{X}}, \mathbf{U} = \begin{pmatrix} \rho \\ \rho u \\ E \end{pmatrix}, \mathbf{F}^{a}(\mathbf{U}) = \begin{pmatrix} \rho u \\ \rho u^{2} + p \\ (E + p)u \end{pmatrix}, \mathbf{F}^{d}(\mathbf{U}, \mathbf{S}) = \frac{1}{\mathsf{Re}} \begin{pmatrix} 0 \\ \tau \\ u\tau + q \end{pmatrix},$$

where  $\tau = \eta u_x$  is shear stress tensor, q is the heat flux given by  $\frac{\gamma}{\Pr} e_x$  and Re is the Reynolds number. The equation of state for ideal gas is  $p = (\gamma - 1)\rho e$ .

By the method in [28,32], a positivity-preserving high order finite volume scheme for (2.6) can be constructed as follows. Let  $\overline{\bf U}_i^n$  denote the approximation to the cell average of the exact solution  ${\bf U}(x,t)$  on the cell  $I_i=[x_{i-\frac{1}{2}},x_{i+\frac{1}{2}}]$  at time level n. A finite volume scheme with forward Euler time discretization can be written as

$$\overline{\mathbf{U}}_{i}^{n+1} = \overline{\mathbf{U}}_{i}^{n} - \frac{\Delta t}{\Delta x} \left[ \widehat{\mathbf{F}}(\mathbf{U}_{i+\frac{1}{2}}^{-}, \mathbf{S}_{i+\frac{1}{2}}^{-}, \mathbf{U}_{i+\frac{1}{2}}^{+}, \mathbf{S}_{i+\frac{1}{2}}^{+}) - \widehat{\mathbf{F}}(\mathbf{U}_{i-\frac{1}{2}}^{-}, \mathbf{S}_{i-\frac{1}{2}}^{-}, \mathbf{U}_{i-\frac{1}{2}}^{+}, \mathbf{S}_{i-\frac{1}{2}}^{+}) \right]$$
(2.7)

with a positivity-preserving flux defined by

$$\widehat{\mathbf{F}}\left(\mathbf{U}_{i+\frac{1}{2}}^{-},\mathbf{S}_{i+\frac{1}{2}}^{-},\mathbf{U}_{i+\frac{1}{2}}^{+},\mathbf{S}_{i+\frac{1}{2}}^{+}\right) = \frac{1}{2}\left[\mathbf{F}\left(\mathbf{U}_{i+\frac{1}{2}}^{-},\mathbf{S}_{i+\frac{1}{2}}^{-}\right) + \mathbf{F}\left(\mathbf{U}_{i+\frac{1}{2}}^{+},\mathbf{S}_{i+\frac{1}{2}}^{+}\right) - \beta_{i+\frac{1}{2}}\left(\mathbf{U}_{i+\frac{1}{2}}^{+} - \mathbf{U}_{i+\frac{1}{2}}^{-}\right)\right],\tag{2.8}$$

where  $\beta_{i+\frac{1}{n}}$  is defined as

$$\beta_{i+\frac{1}{2}} > \max_{\mathbf{U}_{i+\frac{1}{2}}^{\pm}, \mathbf{S}_{i+\frac{1}{2}}^{\pm}} \left[ |u| + \frac{1}{2\rho^2 e} (\sqrt{\rho^2 q^2 + 2\rho^2 e |\tau - p|^2} + \rho |q|) \right]. \tag{2.9}$$

Assume a vector of polynomials of degree k,  $\mathbf{P}_i(x) = (\rho_i(x), m_i(x), E_i(x))^T$ , is a (k+1)-th order accurate approximation to  $\mathbf{U}(x,t)$  in  $I_i$  and satisfies that  $\overline{\mathbf{U}}_i^n$  is the cell average of  $\mathbf{P}_i(x)$  on  $I_i$ , and  $\mathbf{U}_{i-\frac{1}{2}}^+ = \mathbf{P}_i(x_{i-\frac{1}{2}})$ ,  $\mathbf{U}_{i+\frac{1}{2}}^- = \mathbf{P}_i(x_{i+\frac{1}{2}})$ . Denote the N-point Legendre Gauss-Lobatto points on  $I_i$  as  $\{\widehat{\mathbf{x}}_i^\alpha: \alpha=1,2,...,N\} = \{x_{i-\frac{1}{2}}=\widehat{\mathbf{x}}_i^1, \widehat{\mathbf{x}}_i^2, \cdots, \widehat{\mathbf{x}}_i^{N-1}, \widehat{\mathbf{x}}_i^N = x_{i+\frac{1}{2}}\}$  with normalized

quadrature weights  $\widehat{\omega}_{\alpha}$  on the interval  $[-\frac{1}{2},\frac{1}{2}]$  such that  $\sum_{\alpha=1}^{N}\widehat{\omega}_{\alpha}=1$ . The *N*-point Gauss-Lobatto quadrature is exact for integrating polynomials of degree 2N-3. Thus if  $2N-3\geq k$ ,

$$\overline{\mathbf{U}}_{i}^{n} = \frac{1}{\Delta x} \int_{I_{i}} \mathbf{P}_{i}(x) dx = \sum_{\alpha=2}^{N-1} \widehat{\omega}_{\alpha} \mathbf{P}_{i} \left(\widehat{\mathbf{x}}_{j}^{\alpha}\right) + \widehat{\omega}_{1} \mathbf{U}_{i-\frac{1}{2}}^{+} + \widehat{\omega}_{N} \mathbf{U}_{i+\frac{1}{2}}^{-}. \tag{2.10}$$

By the mean value theorem, there exist some points  $x_i^1, x_i^2, x_i^3$  in cell  $I_i$  such that

$$\mathbf{P}_{i}^{*} \equiv \left(\rho_{i}(x_{i}^{1}), m_{i}(x_{i}^{2}), E_{i}(x_{i}^{3})\right)^{T} = \sum_{\alpha=-2}^{N-1} \frac{\widehat{\omega}_{\alpha} \mathbf{P}_{i}\left(\widehat{\mathbf{x}}_{i}^{\alpha}\right)}{1 - \widehat{\omega}_{1} - \widehat{\omega}_{N}} = \frac{\overline{\mathbf{U}}_{i}^{n} - \widehat{\omega}_{1} \mathbf{U}_{i-\frac{1}{2}}^{+} - \widehat{\omega}_{N} \mathbf{U}_{i+\frac{1}{2}}^{-}}{1 - \widehat{\omega}_{1} - \widehat{\omega}_{N}}.$$

$$(2.11)$$

In [28], it has been proven that  $\mathbf{U}_{i\pm\frac{1}{2}}^{\pm}$ ,  $\mathbf{P}_{i}^{*}\in G$  for all i is a sufficient condition for  $\overline{\mathbf{U}}_{i}^{n+1}\in G$  under some suitable CFL condition. A high order accurate limiter for enforcing  $\mathbf{U}_{i\pm\frac{1}{2}}^{\pm}$ ,  $\mathbf{P}_{i}^{*}\in G$  can be used to render the base finite volume scheme positivity-preserving, e.g., [5]. Positivity for high order time discretizations can be achieved by using a strong stability-preserving (SSP) Runge-Kutta method, which is a convex combination of forward Euler steps thus positivity in forward Euler carries over.

#### 3. A positivity-preserving high order finite difference WENO scheme

In this section, we propose a positivity-preserving high order finite difference WENO scheme for solving dimensionless compressible Navier-Stokes equations by interpreting the high order finite difference scheme as a formal high order finite volume scheme, for which a sufficient condition of positive-preserving is obtained and a scaling positivity-preserving limiter can be applied. We first consider forward Euler time discretization and high order time discretizations will be discussed in Section 3.5. When the Navier-Stokes equations reduce to Euler equations, the scheme in this section will reduce to exactly the positivity-preserving finite difference WENO scheme for compressible Euler equations in [34].

#### 3.1. The one-dimensional WENO scheme

For 1D compressible Navier-Stokes equations, consider the following conservative finite difference scheme:

$$\mathbf{U}_{i}^{n+1} = \mathbf{U}_{i}^{n} - \frac{\Delta t}{\Delta x} (\widehat{\mathbf{F}}_{i+\frac{1}{2}} - \widehat{\mathbf{F}}_{i-\frac{1}{2}}), \tag{3.1}$$

where  $\widehat{\mathbf{F}}_{i+\frac{1}{2}}$  is the numerical flux so that  $\frac{1}{\Delta x}(\widehat{\mathbf{F}}_{i+\frac{1}{2}}-\widehat{\mathbf{F}}_{i-\frac{1}{2}})$  is a high order approximation to  $\mathbf{F}(\mathbf{U},\mathbf{S})_x$ , at  $x=x_i,t=t^n$ .

For a (2r+1)-th order finite difference WENO scheme, given point values  $\mathbf{U}_i^n$  at time level n, we first compute  $\mathbf{S}_i^n$  by a (2r+1)-th order finite difference WENO approximation to first order derivatives like in (2.3), (2.4) as described in Section 2.1.

Then for computing  $\hat{\mathbf{F}}_{i+\frac{1}{2}}$  at a given fixed index  $i+\frac{1}{2}$ , we take a positivity-preserving flux splitting to splitted variables in a local stencil,

$$(\mathbf{Z}_{i+\frac{1}{2}}^{\pm})_{j}^{n} = \frac{1}{2} \left( \mathbf{U}_{j}^{n} \pm \frac{\mathbf{F}(\mathbf{U}_{j}^{n}, \mathbf{S}_{j}^{n})}{\beta_{i+\frac{1}{2}}} \right), j = i - r, \dots, i + r + 1,$$
(3.2)

where

$$\beta_{i+\frac{1}{2}} > \max \left[ |u| + \frac{1}{2\rho^2 e} (\sqrt{\rho^2 q^2 + 2\rho^2 e |\tau - p|^2} + \rho |q|) \right], \tag{3.3}$$

and the maximum is taken locally over the WENO reconstruction stencil  $\{i-r,\cdots,i+r+1\}$ . For example, in a fifth order WENO reconstruction, the stencil for computing  $\widehat{\mathbf{F}}_{i+\frac{1}{2}}$  is  $\{i-2,i-1,i,i+1,i+2,i+3\}$ .

We emphasize that  $\beta_{i+\frac{1}{2}}$  has no specific physical meaning, which is the main difference from a Lax-Friedrichs flux splitting for compressible Euler equations in [34]. Let  $A_{i+\frac{1}{2}}$  denote the Roe matrix of the two states  $\mathbf{U}_i^n$  and  $\mathbf{U}_{i+1}^n$ , and  $L_{i+\frac{1}{2}}$  and  $R_{i+\frac{1}{2}}$  denote the left and right eigenvector matrices of  $A_{i+\frac{1}{2}}$ , i.e.,  $A = L\Lambda R$ , where  $\Lambda$  is the diagonal matrix with eigenvalues of A on the diagonal. For each fixed  $x_{i+\frac{1}{2}}$  at time level n, the numerical flux  $\widehat{\mathbf{F}}_{i+\frac{1}{2}}$  can be computed as follows via a characteristic WENO reconstruction.

1. Define  $\mathbf{H}_{i+\frac{1}{2}}^{\pm} = R_{\Delta x}(\mathbf{Z}_{i+\frac{1}{2}}^{\pm})$ , i.e.,

$$\mathbf{Z}_{i+\frac{1}{2}}^{\pm}(\mathbf{U}(x), \mathbf{S}(x)) = \frac{1}{\Delta x} \int_{x-\Delta x/2}^{x+\Delta x/2} \mathbf{H}_{i+\frac{1}{2}}^{\pm}(\eta) d\eta,$$
(3.4)

where  $\mathbf{Z}_{i+\frac{1}{2}}^{\pm}(\mathbf{U}(x),\mathbf{S}(x)) = \frac{1}{2}\left(\mathbf{U} \pm \frac{\mathbf{F}(\mathbf{U},\mathbf{S})}{\beta_{i+\frac{1}{2}}}\right)$ . Then we have the cell averages

$$(\overline{\mathbf{H}_{i+\frac{1}{2}}^{\pm}})_{j}^{n} = (\mathbf{Z}_{i+\frac{1}{2}}^{\pm})_{j}^{n}, \quad j = i-r, \cdots, i+r+1.$$

2. Transform the cell averages  $(\overline{\mathbf{H}_{i+\frac{1}{2}}^{\pm}})_{j}^{n}$  from physical space to the local characteristic space by

$$(\overline{\mathbf{T}_{i+\frac{1}{2}}^{\pm}})_{j}^{n} = L_{i+\frac{1}{2}}(\overline{\mathbf{H}_{i+\frac{1}{2}}^{\pm}})_{j}^{n}, \quad j = i-r, \cdots, i+r+1.$$

3. Perform the WENO reconstruction for each component of  $(\overline{\mathbf{T}_{i+\frac{1}{2}}^+})_j^n$  to obtain approximations of the point value of the function  $L_{i+\frac{1}{2}}\mathbf{H}_{i+\frac{1}{2}}^+$  at  $x_{i+\frac{1}{2}}$ , denoted by  $(\mathbf{T}_{i+\frac{1}{2}}^+)_{i+\frac{1}{2}}^\pm$ , where the superscripts  $\pm$  outside of the parentheses of  $(\mathbf{T}_{i+\frac{1}{2}}^+)_{i+\frac{1}{2}}^\pm$  denote approximations from the right and from the left respectively. Perform the WENO reconstruction for each component of  $(\overline{\mathbf{T}_{i+\frac{1}{2}}^-})_j^n$  to obtain approximations of the point value of the function  $L_{i+\frac{1}{2}}\mathbf{H}_{i+\frac{1}{2}}^-$  at  $x_{i+\frac{1}{2}}$ , denoted by  $(\mathbf{T}_{i+\frac{1}{2}}^-)_{i+\frac{1}{2}}^\pm$ .

4. Transform back into physical space by

$$(\mathbf{H}_{i+\frac{1}{2}}^{+})_{i+\frac{1}{2}}^{-} = R_{i+\frac{1}{2}}(\mathbf{T}_{i+\frac{1}{2}}^{+})_{i+\frac{1}{2}}^{-}, \quad (\mathbf{H}_{i+\frac{1}{2}}^{-})_{i+\frac{1}{2}}^{+} = R_{i+\frac{1}{2}}(\mathbf{T}_{i+\frac{1}{2}}^{-})_{i+\frac{1}{2}}^{+}.$$

5. Obtain the numerical flux by

$$\widehat{\mathbf{F}}_{i+\frac{1}{2}} = \beta_{i+\frac{1}{2}} [(\mathbf{H}_{i+\frac{1}{2}}^+)_{i+\frac{1}{2}}^- - (\mathbf{H}_{i+\frac{1}{2}}^-)_{i+\frac{1}{2}}^+]. \tag{3.5}$$

**Remark 3.1.** For the ease of understanding subscripts and superscripts, we give a further explanation. The superscripts  $\pm$  in  $\mathbf{Z}_{i+\frac{1}{2}}^{\pm}$  denote the positive and negative in the flux splitting (3.2). For  $(\mathbf{H}_{i+\frac{1}{2}}^{\pm})_j^n$ ,  $(\mathbf{T}_{i+\frac{1}{2}}^{\pm})_j^n$ ,  $(\mathbf{H}_{i+\frac{1}{2}}^{\pm})_{i+\frac{1}{2}}^{\pm}$ ,  $(\mathbf{T}_{i+\frac{1}{2}}^{\pm})_{i+\frac{1}{2}}^{\pm}$ , the superscripts  $\pm$  inside of the parentheses also denote the positive and negative flux splitting. For  $(\mathbf{H}_{i+\frac{1}{2}}^{\pm})_{i+\frac{1}{2}}^{\pm}$ ,  $(\mathbf{T}_{i+\frac{1}{2}}^{\pm})_{i+\frac{1}{2}}^{\pm}$ , their superscripts  $\pm$  outside of the parentheses denote approximations from the right and left of point  $x_{i+\frac{1}{2}}$  respectively. All subscripts  $i+\frac{1}{2}$  inside the parentheses emphasize that the reconstruction is performed for splitted variables  $\mathbf{Z}_{i+\frac{1}{2}}$  which depends on  $\beta_{i+\frac{1}{2}}$ , while subscripts  $i+\frac{1}{2}$  outside of the parentheses represent point values at  $x_{i+\frac{1}{2}}$ .

#### 3.2. Sufficient conditions for positivity

Next, we will derive a sufficient condition for the scheme (3.1) to keep  $\mathbf{U}_i^{n+1} \in G$  if  $\mathbf{U}_i^n \in G$ .

For a fixed i, we have  $\mathbf{U}_{i}^{n} = (\overline{\mathbf{H}_{i+\frac{1}{2}}^{+}})_{i}^{n} + (\overline{\mathbf{H}_{i+\frac{1}{2}}^{-}})_{i}^{n} = (\overline{\mathbf{H}_{i-\frac{1}{2}}^{+}})_{i}^{n} + (\overline{\mathbf{H}_{i-\frac{1}{2}}^{-}})_{i}^{n}$  from (3.2). Plugging it into (3.5) and (3.1), we can get

$$\mathbf{U}_{i}^{n+1} = \mathbf{U}_{i}^{n} - \frac{\Delta t}{\Delta x} (\widehat{\mathbf{F}}_{i+\frac{1}{2}} - \widehat{\mathbf{F}}_{i-\frac{1}{2}}) = \mathbf{H}_{1} + \mathbf{H}_{2}$$
(3.6)

with

$$\mathbf{H}_{1} = \frac{1}{2} (\overline{\mathbf{H}_{i+\frac{1}{2}}^{+}})_{i}^{n} + \frac{1}{2} (\overline{\mathbf{H}_{i+\frac{1}{2}}^{-}})_{i}^{n} - \frac{\Delta t}{\Delta x} \beta_{i+\frac{1}{2}} (\mathbf{H}_{i+\frac{1}{2}}^{+})_{i+\frac{1}{2}}^{-} + \frac{\Delta t}{\Delta x} \beta_{i+\frac{1}{2}} (\mathbf{H}_{i+\frac{1}{2}}^{-})_{i+\frac{1}{2}}^{+},$$

$$(3.7)$$

$$\mathbf{H}_{2} = \frac{1}{2} (\overline{\mathbf{H}_{i-\frac{1}{2}}^{+}})_{i}^{n} + \frac{1}{2} (\overline{\mathbf{H}_{i-\frac{1}{2}}^{-}})_{i}^{n} + \frac{\Delta t}{\Delta x} \beta_{i-\frac{1}{2}} (\mathbf{H}_{i-\frac{1}{2}}^{+})_{i-\frac{1}{2}}^{-} - \frac{\Delta t}{\Delta x} \beta_{i-\frac{1}{2}} (\mathbf{H}_{i-\frac{1}{2}}^{-})_{i-\frac{1}{2}}^{+}.$$

$$(3.8)$$

It suffices to discuss conditions to keep  $\mathbf{H}_1, \mathbf{H}_2 \in G$ . If given  $\mathbf{U}_i^n \in G$  at time level n, then  $(\overline{\mathbf{H}_{i+\frac{1}{2}}^{\pm}})_j^n = (\mathbf{Z}_{i+\frac{1}{2}}^{\pm})_j^n = \frac{1}{2}(\mathbf{U}_i^n \pm \beta_{i+\frac{1}{2}}^{-1}\mathbf{F}(\mathbf{U}_i^n, \mathbf{S}_i^n)) \in G$ , which was proved in Lemma 6 of [28]. We first discuss  $\mathbf{H}_1$  in equation (3.7).

By interpolation [30], there exists a vector of polynomials of degree k = 2r, denoted  $\mathbf{P}_{i}^{+}(x)$ , satisfying

1. the cell average of  $\mathbf{P}_{i}^{+}(x)$  on the interval  $I_{i}$  is  $(\overline{\mathbf{H}_{i+\frac{1}{2}}^{+}})_{i}^{n}$ ;

- 2.  $\mathbf{P}_{i}^{+}(x_{i+\frac{1}{2}}) = (\mathbf{H}_{i+\frac{1}{2}}^{+})_{i+\frac{1}{2}}^{-};$
- 3.  $\mathbf{P}_{i}^{+}(x)$  is a (2r+1)-th order accurate approximation to the function  $\mathbf{H}_{i+\frac{1}{2}}^{+}(x)$  on the interval  $I_{i}$  if  $\mathbf{H}_{i+\frac{1}{2}}^{+}(x)$  is smooth.

Recall that we have reviewed quadrature in Section 2.2. Let  $N = \lceil \frac{2r+3}{2} \rceil$ , i.e., N is the smallest integer s.t.  $N \ge \frac{2r+3}{2}$ , then the exactness of the Gauss-Lobatto quadrature rule implies

$$(\overline{\mathbf{H}_{i+\frac{1}{2}}^{+}})_{i}^{n} = \frac{1}{\Delta x} \int_{I_{i}} \mathbf{P}_{i}^{+}(x) dx = \sum_{\alpha=1}^{N} \widehat{\omega}_{\alpha} \mathbf{P}_{i}^{+}(\widehat{\mathbf{x}}_{j}^{\alpha}) = (1 - \widehat{\omega}_{N}) \mathbf{P}_{i}^{+,*} + \widehat{\omega}_{N} (\mathbf{H}_{i+\frac{1}{2}}^{+})_{i+\frac{1}{2}}^{-},$$

where

$$\mathbf{P}_{i}^{+,*} = \frac{1}{1 - \widehat{\omega}_{N}} \sum_{\alpha=1}^{N-1} \widehat{\omega}_{\alpha} \mathbf{P}_{i}^{+} (\widehat{\mathbf{x}}_{j}^{\alpha}) = \frac{1}{1 - \widehat{\omega}_{N}} [(\overline{\mathbf{H}}_{i+\frac{1}{2}}^{+})_{i}^{n} - \widehat{\omega}_{N} (\mathbf{H}_{i+\frac{1}{2}}^{+})_{i+\frac{1}{2}}^{-}].$$

We have

$$\mathbf{H}_{1} = \frac{1}{2} (\overline{\mathbf{H}_{i+\frac{1}{2}}^{-}})_{i}^{n} + \frac{1 - \widehat{\omega}_{N}}{2} \mathbf{P}_{i}^{+,*} + (\frac{\widehat{\omega}_{N}}{2} - \frac{\Delta t}{\Delta x} \beta_{i+\frac{1}{2}}) (\mathbf{H}_{i+\frac{1}{2}}^{+})_{i+\frac{1}{2}}^{-} + \frac{\Delta t}{\Delta x} \beta_{i+\frac{1}{2}} (\mathbf{H}_{i+\frac{1}{2}}^{-})_{i+\frac{1}{2}}^{+}.$$

So under the CFL condition  $\frac{\Delta t}{\Delta x}\beta_{i+\frac{1}{2}} \leq \frac{1}{2}\widehat{\omega}_N$ , if  $\mathbf{U}_i^n$ ,  $\mathbf{P}_i^{+,*}$ ,  $(\mathbf{H}_{i+\frac{1}{2}}^+)_{i+\frac{1}{2}}^-$ ,  $(\mathbf{H}_{i+\frac{1}{2}}^+)_{i+\frac{1}{2}}^+$   $\in G$ , then we have  $\mathbf{H}_1 \in G$  because it is a convex combination of four vectors in G.

Similarly, discussion for  $H_2$  in equation (3.8). By interpolation [30], there exists a vector of polynomials of degree k = 2r, denoted  $\mathbf{P}_{i}^{-}(x)$ , satisfying

- 1. the cell average of  $\mathbf{P}_i^-(x)$  on the interval  $I_i$  is  $(\overline{\mathbf{H}_{i-1}^-})_i^n$ ;
- 2.  $\mathbf{P}_{i}^{-}(x_{i-\frac{1}{2}}) = (\mathbf{H}_{i-\frac{1}{2}}^{-})_{i-\frac{1}{2}}^{+};$
- 3.  $\mathbf{P}_{i}^{-}(x)$  is a (2r+1)-th order accurate approximation to the function  $\mathbf{H}_{i-\frac{1}{2}}^{-}(x)$  on the interval  $I_{i}$  if  $\mathbf{H}_{i-\frac{1}{2}}^{-}(x)$  is smooth.

The quadrature rule implies

$$(\overline{\mathbf{H}_{i-\frac{1}{2}}^{-}})_{i}^{n} = \frac{1}{\Delta x} \int_{I_{i}} \mathbf{P}_{i}^{-}(x) dx = \sum_{\alpha=1}^{N} \widehat{\omega}_{\alpha} \mathbf{P}_{i}^{-}(\widehat{x}_{j}^{\alpha}) = \widehat{\omega}_{1} (\mathbf{H}_{i-\frac{1}{2}}^{-})_{i-\frac{1}{2}}^{+} + (1-\widehat{\omega}_{1}) \mathbf{P}_{i}^{-,*},$$

where

$$\mathbf{P}_i^{-,*} = \frac{1}{1 - \widehat{\omega}_1} \sum_{\alpha = 2}^N \widehat{\omega}_\alpha \mathbf{P}_i^{-}(\widehat{\mathbf{X}}_j^\alpha) = \frac{1}{1 - \widehat{\omega}_1} [(\overline{\mathbf{H}_{i-\frac{1}{2}}^-})_i^n - \widehat{\omega}_1 (\mathbf{H}_{i-\frac{1}{2}}^-)_{i-\frac{1}{2}}^+].$$

We have

$$\mathbf{H}_2 = \frac{1}{2} (\overline{\mathbf{H}_{i-\frac{1}{2}}^+})_i^n + \frac{1-\widehat{\omega}_1}{2} \mathbf{P}_i^{-,*} + (\frac{\widehat{\omega}_1}{2} - \frac{\Delta t}{\Delta x} \beta_{i-\frac{1}{2}}) (\mathbf{H}_{i-\frac{1}{2}}^-)_{i-\frac{1}{2}}^+ + \frac{\Delta t}{\Delta x} \beta_{i-\frac{1}{2}} (\mathbf{H}_{i-\frac{1}{2}}^+)_{i-\frac{1}{2}}^-.$$

So under the CFL condition  $\frac{\Delta t}{\Delta x}\beta_{i-\frac{1}{2}} \leq \frac{1}{2}\widehat{\omega}_1$ , if  $\mathbf{U}_i^n, \mathbf{P}_i^{-,*}, (\mathbf{H}_{i-\frac{1}{2}}^-)_{i-\frac{1}{2}}^+, (\mathbf{H}_{i-\frac{1}{2}}^+)_{i-\frac{1}{2}}^- \in G$ , then  $\mathbf{H}_2 \in G$  because it is a convex combination of four vectors in G. Notice that  $\widehat{\omega}_1 = \widehat{\omega}_N = \frac{1}{N(N-1)}$ . By above discussion, we have the following main result.

**Theorem 1.** The (2r+1)-th order accurate finite difference WENO scheme (3.1) and (3.5) is positivity-preserving, i.e.,  $\mathbf{U}_i^n \in G \Rightarrow$  $\mathbf{U}_i^{n+1} \in G$ , if

$$\mathbf{P}_{i}^{+,*}, (\mathbf{H}_{i+\frac{1}{2}}^{+})_{i+\frac{1}{2}}^{-}, (\mathbf{H}_{i+\frac{1}{2}}^{-})_{i+\frac{1}{2}}^{+}, \mathbf{P}_{i}^{-,*}, (\mathbf{H}_{i-\frac{1}{2}}^{-})_{i-\frac{1}{2}}^{+}, (\mathbf{H}_{i-\frac{1}{2}}^{+})_{i-\frac{1}{2}}^{-} \in G, \quad \forall i$$

$$(3.9)$$

under the CFL condition

$$\frac{\Delta t}{\Delta x} \max_{i} \beta_{i+\frac{1}{2}} \le \frac{1}{2N(N-1)},\tag{3.10}$$

where  $N = \lceil \frac{2r+3}{2} \rceil$  and

$$\mathbf{P}_{i}^{+,*} = \frac{(\overline{\mathbf{H}_{i+\frac{1}{2}}^{+}})_{i+\frac{1}{2},i}^{n} - \widehat{\omega}_{N}(\mathbf{H}_{i+\frac{1}{2}}^{+})_{i+\frac{1}{2}}^{-}}{1 - \widehat{\omega}_{N}}, \mathbf{P}_{i}^{-,*} = \frac{(\overline{\mathbf{H}_{i-\frac{1}{2}}^{-}})_{i-\frac{1}{2},i}^{n} - \widehat{\omega}_{1}(\mathbf{H}_{i-\frac{1}{2}}^{-})_{i-\frac{1}{2}}^{+}}{1 - \widehat{\omega}_{1}}.$$
(3.11)

**Remark 3.2.** The polynomials  $P_i^{\pm}(x)$  are needed only for deriving sufficient conditions for positivity, but they are not needed and never used in the implementation.

**Remark 3.3.** The sufficient condition in Theorem 1 is an intrinsic property of any finite difference scheme interpreted as a finite volume scheme for an auxiliary variable. On the other hand, we emphasize that Theorem 1 is a weak positivity result, i.e., the scheme (3.1) and (3.5) is not positivity-preserving unless (3.9) is enforced by additional limiters. Moreover, the CFL (3.10) is only sufficient but not always necessary for positivity. For a smooth solution the CFL (3.10) reduces to  $\Delta t = \mathcal{O}(\Delta x)$ , which does not satisfy the linear stability CFL  $\Delta t = \mathcal{O}(\text{Re}\Delta x^2)$  in an explicit scheme for a convection diffusion problem [28]. In practice,  $\Delta t = \mathcal{O}(\text{Re}\Delta x^2)$  should be always obeyed in the WENO scheme, and (3.10) should be enforced only when positivity is lost. See Section 3.5 for details.

#### 3.3. A high order accurate positivity-preserving limiter

To enforce the condition (3.9) in Theorem 1, we can simply use the limiter in [34], which is essentially the same as applying the high order accurate positivity-preserving limiter in [28] to two formal finite volume schemes (3.7) and (3.8). For simplicity, let  $(\overline{\mathbf{H}_{i+\frac{1}{2}}^+})_i^n = (\overline{\rho}_i, \overline{m}_i, \overline{E}_i)^T$ ,  $(\mathbf{H}_{i+\frac{1}{2}}^+)_{i+\frac{1}{2}}^- = (\rho_{i+\frac{1}{2}}^-, m_{i+\frac{1}{2}}^-, E_{i+\frac{1}{2}}^-)^T$  and  $\mathbf{P}_i^{+,*} = (\rho_i^*, m_i^*, E_i^*,)^T$ . The following limiter procedures can enforce the condition (3.9) in Theorem 1.

For a fixed index  $i + \frac{1}{2}$ , we apply the following limiter:

Step 1. Setup a small positivity number  $\varepsilon$  as a desired lower bound for density and internal energy, e.g.,  $\varepsilon = \min\left\{10^{-13}, \rho\left((\overline{\mathbf{H}_{i+\frac{1}{2}}^+})_i^n\right)\right\}$ . Step 2. For each cell  $I_i = [x_{i-\frac{1}{2}}, x_{i+\frac{1}{2}}]$ , we first modify density by

$$\hat{\rho}_{i+\frac{1}{2}}^{-} = \theta_{\rho} \left( \rho_{i+\frac{1}{2}}^{-} - \bar{\rho}_{i} \right) + \bar{\rho}_{i}, \quad \theta_{\rho} = \min \left\{ 1, \frac{\bar{\rho}_{i} - \varepsilon}{\bar{\rho}_{i} - \rho_{min}} \right\}, \tag{3.12}$$

where 
$$\rho_{min} = \min\left\{\rho_{i+\frac{1}{2}}^-, \rho_i^*\right\}$$
. Then denote  $(\widehat{\mathbf{H}}_{i+\frac{1}{2}}^+)_{i+\frac{1}{2}}^- = (\widehat{\rho}_{i+\frac{1}{2}}^-, m_{i+\frac{1}{2}}^-, E_{i+\frac{1}{2}}^-)^T$  and  $\widehat{\mathbf{P}}_i^{+,*} = \frac{1}{1-\widehat{\omega}_N}\left[(\overline{\mathbf{H}}_{i+\frac{1}{2}}^+)_i^n - \widehat{\omega}_N(\widehat{\mathbf{H}}_{i+\frac{1}{2}}^+)_{i+\frac{1}{2}}^-\right]$ .

Step 3. For convenience, let  $\widehat{\mathbf{q}}_1 = (\widehat{\mathbf{H}}_{i+\frac{1}{2}}^+)_{i+\frac{1}{2}}^-$ ,  $\widehat{\mathbf{q}}_2 = \widehat{\mathbf{P}}_i^{+,*}$ . Define  $\overline{\rho e}_i = \overline{E}_i - \frac{1}{2} \frac{\overline{m}_i^2}{\overline{\rho_i}}$  For k = 1, 2, compute

$$t_{\varepsilon}^{k} = \begin{cases} \frac{\overline{\rho e_{i}} - \varepsilon}{\overline{\rho e_{i}} - \rho e(\widehat{\mathbf{q}}_{k})}, & \text{if } \rho e(\widehat{\mathbf{q}}_{k}) < \varepsilon \\ 1, & \text{if } \rho e(\widehat{\mathbf{q}}_{k}) \ge \varepsilon \end{cases}$$

Then we modify the internal energy by

$$(\widetilde{\mathbf{H}}_{i+\frac{1}{2}}^{+})_{i+\frac{1}{2}}^{-} = \theta_{e} \left( (\widehat{\mathbf{H}}_{i+\frac{1}{2}}^{+})_{i+\frac{1}{2}}^{-} - (\overline{\mathbf{H}}_{i+\frac{1}{2}}^{+})_{i}^{n} \right) + (\overline{\mathbf{H}}_{i+\frac{1}{2}}^{+})_{i}^{n}, \quad \theta_{e} = \min\{t_{\varepsilon}^{1}, t_{\varepsilon}^{2}\}.$$

$$(3.13)$$

Similarly, we can get the revised point value  $(\widetilde{\mathbf{H}}_{i+\frac{1}{2}}^-)_{i+\frac{1}{2}}^+$ . Finally, we have the modified WENO flux with

$$\widehat{\mathbf{F}}_{i+\frac{1}{2}} = \beta_{i+\frac{1}{2}} [(\widetilde{\mathbf{H}}_{i+\frac{1}{2}}^{+})_{i+\frac{1}{2}}^{-} - (\widetilde{\mathbf{H}}_{i+\frac{1}{2}}^{-})_{i+\frac{1}{2}}^{+}]. \tag{3.14}$$

By Theorem 1, the modified scheme (3.1) and (3.14) is positivity-preserving.

This limiter is high order accurate for smooth solutions without vacuum in the following asymptotic sense. Assume the exact smooth solution  $\mathbf{U}(x,t)$  has a uniform lower bound in density and internal energy, i.e.,

$$\min_{x,t} \rho(\mathbf{U}(x,t)) = a > 0, \min_{x,t} \rho e(\mathbf{U}(x,t)) = b > 0.$$

By Lemma 6 in [28], with suitable  $\beta_{i+\frac{1}{2}}$ , we have  $\mathbf{Z}_{i+\frac{1}{2}}^{\pm} \in G$ . If  $\Delta x$  is small enough,  $\mathbf{H}_{i+\frac{1}{2}}^{\pm}$  defined in (3.4) satisfies  $\mathbf{H}_{i+\frac{1}{2}}^{\pm} \in G$ . Notice that the limiter (3.12) and (3.13) are exactly the same type of limiter for finite volume scheme (3.7) as in [28]. Based the same arguments in [28], if regarding it as a limiter applied to polynomials approximating the auxiliary function  $\mathbf{H}_{+i+1}$ , it is straightforward to show that the scaling positivity-preserving limiter will not destroy the high order accuracy of the finite difference WENO schemes for smooth solutions without vacuum regions when  $\Delta x$  is small, see also [34].

We summarize the implementation of positivity-preserving finite difference WENO in Algorithm 1.

#### **Algorithm 1** Implementation of positivity-preserving finite difference WENO.

**Input:** Point values  $\mathbf{U}_i^n \in G$ ,  $i = -r, \dots, N_x + r + 1$ , where  $N_x$  is number of grid-point.

**Output:** Numerical flux  $\hat{\mathbf{F}}_{i+\frac{1}{x}}$ ,  $i = 0, \dots, N_x$ .

- 1: **Step I** Compute the derivative values  $S_i^n$  by the 2r + 1 order WENO reconstruction.
- 2: **Step II** Compute the flux splitting  $(\mathbf{Z}_{i+\frac{1}{2}}^{\pm i})_{j}^{n}$  by (3.2).
- 3: **Step III** Compute  $(\mathbf{H}_{i+\frac{1}{2}}^+)_{i+\frac{1}{2}}^-$  and  $(\mathbf{H}_{i+\frac{1}{2}}^-)_{i+\frac{1}{2}}^+$  by the 2r+1 order WENO reconstruction. 4: **Step IV** Compute  $(\widetilde{\mathbf{H}}_{i+\frac{1}{2}}^+)_{i+\frac{1}{2}}^-$  and  $(\widetilde{\mathbf{H}}_{i+\frac{1}{2}}^-)_{i+\frac{1}{2}}^+$  by the positivity-preserving limiter.
- 5: **Step IV** Compute the numerical flux  $\hat{\mathbf{F}}_{i+\frac{1}{n}}$  by (3.14).

#### 3.4. Two-dimensional case

Consider the dimensionless form of compressible dimensionless Navier-Stokes equations

$$\mathbf{U}_t + \nabla \cdot \mathbf{F}^a = \nabla \cdot \mathbf{F}^d, \tag{3.15}$$

where  $\mathbf{U} = (\rho, \rho \mathbf{u}, E)^T$  are the conservative variables,  $\rho$  is the density,  $\mathbf{u} = (u, v)$ , u and v denote the velocity in x and ydirection respectively, E is the total energy, the flux function  $\mathbf{F}^a$  and  $\mathbf{F}^d$  are respect to advection and diffusion fluxes

$$\mathbf{F}^{d} = \begin{pmatrix} \rho \mathbf{u} \\ \rho \mathbf{u} \otimes \mathbf{u} + p \mathbb{I} \\ (E+p)\mathbf{u} \end{pmatrix}, \quad \mathbf{F}^{d} = \begin{pmatrix} 0 \\ \mathbf{\tau} \\ \mathbf{u} \cdot \mathbf{\tau} - \mathbf{q} \end{pmatrix}, \tag{3.16}$$

where  ${\mathbb I}$  is the unit tensor, the shear stress tensor and heat diffusion flux are

$$\tau = \frac{1}{\text{Re}} \begin{pmatrix} \tau_{xx} & \tau_{xy} \\ \tau_{yx} & \tau_{yy} \end{pmatrix}, \quad \mathbf{q} = \frac{1}{\text{Re}} \frac{\gamma}{\text{Pr}} (e_x, e_y)^T$$
(3.17)

with  $\tau_{xx} = \frac{4}{3}u_x - \frac{2}{3}v_y$ ,  $\tau_{xy} = \tau_{yx} = u_y + v_x$ ,  $\tau_{yy} = \frac{4}{3}v_y - \frac{2}{3}u_x$ . The total energy is  $E = \frac{p}{\gamma - 1} + \frac{1}{2}\rho u^2 + \frac{1}{2}\rho v^2$  and EOS is  $p = (\gamma - 1)\rho e$ , where p is the pressure and e is the internal energy. Denote  $\mathbf{S} = \nabla \mathbf{U}$ . We can regard  $\mathbf{F}^a - \mathbf{F}^d$  as a single flux and formally treat  $\nabla \cdot (\mathbf{F}^a - \mathbf{F}^d)$  as a convection by combining the advection flux  $\mathbf{F}^a$  and diffusion flux  $\mathbf{F}^d$ , then (3.15) can be

$$\mathbf{U}_t + \mathbf{F}(\mathbf{U}, \mathbf{S})_x + \mathbf{G}(\mathbf{U}, \mathbf{S})_y = 0 \tag{3.18}$$

with

$$\mathbf{F}(\mathbf{U}, \mathbf{S}) = \begin{bmatrix} \rho u \\ \rho u^2 + p - \frac{1}{Re} \tau_{xx} \\ \rho u v - \frac{1}{Re} \tau_{yx} \\ (E + p) u - \frac{1}{Re} (\tau_{xx} u + \tau_{yx} v + \frac{\gamma e_x}{Pr}) \end{bmatrix},$$

$$\mathbf{G}(\mathbf{U}, \mathbf{S}) = \begin{bmatrix} \rho v \\ \rho u v - \frac{1}{Re} \tau_{xy} \\ \rho v^2 + p - \frac{1}{Re} \tau_{yy} \\ (E + p) v - \frac{1}{Pe} (\tau_{xy} u + \tau_{yy} v + \frac{\gamma e_y}{Pr}) \end{bmatrix}.$$

Consider a uniform grid with nodes  $(x_i, y_i)$ . A conservative WENO finite difference with forward Euler discretization can be written as

$$\mathbf{U}_{ij}^{n+1} = \mathbf{U}_{ij}^{n} - \frac{\Delta t}{\Delta x} (\widehat{\mathbf{F}}_{i+\frac{1}{2},j} - \widehat{\mathbf{F}}_{i-\frac{1}{2},j}) - \frac{\Delta t}{\Delta y} (\widehat{\mathbf{G}}_{i,j+\frac{1}{2}} - \widehat{\mathbf{G}}_{i,j-\frac{1}{2}}). \tag{3.19}$$

We use the same positivity-preserving flux splitting,

$$\mathbf{Z}_{i+\frac{1}{2},j}^{\pm}(\mathbf{U},\mathbf{S}) = \frac{1}{2} \left( \mathbf{U} \pm \frac{\mathbf{F}(\mathbf{U},\mathbf{S})}{\beta_{i+\frac{1}{2},j}^{x}} \right), \quad \mathbf{Z}_{i,j+\frac{1}{2}}^{\pm}(\mathbf{U},\mathbf{S}) = \frac{1}{2} \left( \mathbf{U} \pm \frac{\mathbf{G}(\mathbf{U},\mathbf{S})}{\beta_{i,j+\frac{1}{2}}^{y}} \right),$$
(3.20)

$$\beta_{i+\frac{1}{2},j}^{x} > \max \left[ |\mathbf{u} \cdot \mathbf{n}_{1}| + \frac{1}{2\rho^{2}e} (\sqrt{\rho^{2} |\mathbf{q} \cdot \mathbf{n}_{1}|^{2} + 2\rho^{2}e \|\boldsymbol{\tau} \cdot \mathbf{n}_{1} - p\mathbf{n}_{1}\|^{2}} + \rho |\mathbf{q} \cdot \mathbf{n}_{1}|) \right], \tag{3.21}$$

$$\beta_{i,j+\frac{1}{2}}^{y} > \max \left[ |\mathbf{u} \cdot \mathbf{n}_{2}| + \frac{1}{2\rho^{2}e} (\sqrt{\rho^{2} |\mathbf{q} \cdot \mathbf{n}_{2}|^{2} + 2\rho^{2}e \|\boldsymbol{\tau} \cdot \mathbf{n}_{2} - p\mathbf{n}_{2}\|^{2}} + \rho |\mathbf{q} \cdot \mathbf{n}_{2}|) \right], \tag{3.22}$$

#### Algorithm 2 Implementation of the time discretization.

```
Input: point values \mathbf{U}^n \in G.
 Output: point values \mathbf{U}^{n+1} \in G.
 1: Step I Compute the wave speed \alpha_i = |u_i| + \sqrt{\frac{\gamma p_i}{a_i}}. Let \alpha^* = \max_i |\alpha_i|. Set up time step \Delta t = \min\{a\frac{\Delta x}{\alpha^*}, b \operatorname{Re} \Delta x^2\} with the two parameters a = 0.6 and
 2: Step II Compute \mathbf{U}^{(1)} = \mathbf{U}^n + \Delta t \mathcal{L}(\mathbf{U}^n).
 3: if \mathbf{U}^{(1)} \in G then
          Proceed to next Step III;
           Setup time step \Delta t = \frac{\Delta t}{2} and restart the computation.
 6:
  7: Step III Compute \mathbf{U}^{(2)} = \frac{3}{4}\mathbf{U}^n + \frac{1}{4}(\mathbf{U}^{(1)} + \Delta t \mathcal{L}(\mathbf{U}^{(1)})).
 8: if U^{(2)} \in G then
          proceed to next step Step IV;
10: else
           Setup time step \Delta t = \frac{\Delta t}{2}, return to Step II and restart the computation.
11:
12: Step IV Compute \mathbf{U}^{n+1} = \frac{1}{3}\mathbf{U}^n + \frac{2}{3}(\mathbf{U}^{(2)} + \Delta t \mathcal{L}(\mathbf{U}^{(2)})).
13: if U^{(1)} \in G then
           The computation to step n + 1 is done;
15: else
           Setup time step \Delta t = \frac{\Delta t}{2}, return to Step II and restart the computation.
16:
17: return
```

where the maximum is taken locally over the corresponding WENO stencils and  $\mathbf{n}_1 = (1,0)^T$ ,  $\mathbf{n}_2 = (0,1)^T$ . According to the Lemma 6 in [28], it is easy to check that  $\mathbf{Z}_{i+\frac{1}{2},j}^{\pm}(\mathbf{U},\mathbf{S})$ ,  $\mathbf{Z}_{i,j+\frac{1}{2}}^{\pm}(\mathbf{U},\mathbf{S}) \in G$  if  $\mathbf{U} \in G$ . The numerical flux  $\widehat{\mathbf{F}}_{i+\frac{1}{2},j}$  and  $\widehat{\mathbf{G}}_{i,j+\frac{1}{2}}$  in (3.19) can be obtained by the dimension-by-dimension reconstruction in exactly the same way of one-dimensional WENO approximation. For the property of positivity-preserving in (3.19), we rewrite the scheme as  $\mathbf{U}_{ij}^{n+1} = \frac{1}{2}\mathbf{F} + \frac{1}{2}\mathbf{G}$  with

$$\mathbf{F} = \mathbf{U}_{ij}^{n} - 2\frac{\Delta t}{\Delta x} \left( \widehat{\mathbf{F}}_{i+\frac{1}{2},j} - \widehat{\mathbf{F}}_{i-\frac{1}{2},j} \right), \quad \mathbf{G} = \mathbf{U}_{ij}^{n} - 2\frac{\Delta t}{\Delta x} \left( \widehat{\mathbf{G}}_{i,j+\frac{1}{2}} - \widehat{\mathbf{G}}_{i,j-\frac{1}{2}} \right). \tag{3.23}$$

If  $\mathbf{F}, \mathbf{G} \in G$ , then  $\mathbf{U}_{ij}^{n+1} \in G$ . Notice that (3.23) are two formal one-dimensional schemes, thus Theorem 1 applies to both  $\mathbf{F}$  and  $\mathbf{G}$ . So it is straightforward to extend the one-dimension positivity-preserving results and the limiter to two-dimensions.

#### 3.5. High order time discretizations and implementation details

For high order time discretizations, we can use any high order strong stability-preserving (SSP) Runge-Kutta method, which is a convex combination of forward Euler steps, thus all discussion about positivity for forward Euler still holds due to convex combinations since the set G is convex. In numerical tests, we use the third order SSP Runge-Kutta method. For solving  $\frac{d}{dt}\mathbf{U} = \mathcal{L}(\mathbf{U})$ , it can be written as

$$\begin{cases}
\mathbf{U}^{(1)} = \mathbf{U}^{n} + \Delta t \mathcal{L}(\mathbf{U}^{n}), \\
\mathbf{U}^{(2)} = \frac{3}{4} \mathbf{U}^{n} + \frac{1}{4} (\mathbf{U}^{(1)} + \Delta t \mathcal{L}(\mathbf{U}^{(1)})), \\
\mathbf{U}^{n+1} = \frac{1}{3} \mathbf{U}^{n} + \frac{2}{3} (\mathbf{U}^{(2)} + \Delta t \mathcal{L}(\mathbf{U}^{(2)})).
\end{cases} (3.24)$$

The time step should not be set as the CFL (3.10) because it gives  $\Delta t = \mathcal{O}(\Delta x)$  for smooth solutions which is inconsistent with linear stability constraints  $\Delta t = \mathcal{O}(\text{Re}\Delta x^2)$ . For a solution with shocks but far away from vacuum, the CFL (3.10) is much stringent than a necessary time step for positivity in WENO schemes. So for the sake of efficiency, (3.10) should not always be enforced either. To this end, (3.10) should be enforced only when positivity is lost, and we can use the same simple time marching strategy in [28]. The positivity-preserving limiter should be used for each stage in (3.24). The positivity-preserving high order finite difference WENO schemes with the third order SSP Runge-Kutta (3.24) for equation (3.1) are implemented as in the Algorithm 2.

**Remark 3.4.** Obviously one can use the Algorithm 2. for any finite difference scheme, but the restarting might result in an infinite loop. Even though the CFL (3.10) is never used directly in the Algorithm 2, Theorem 1 ensures that it will not be an infinite loop in the positivity-preserving scheme since the restarting will end when (3.10) is satisfied for each forward Euler step.

**Remark 3.5.** Theorem 1 will hold for any method computing point values of derivatives  $S = \nabla U$ . But Theorem 1 is only about positivity and a positivity-preserving scheme can still be oscillatory [28]. In our numerical tests, we find that a high order linear approximation for approximating derivatives  $u_x$  and  $e_x$  can result in oscillations. Instead, given point values of U, we

use high order WENO finite difference approximation to find point values of  $\mathbf{S} = \nabla U$ . After derivatives of conserved variables  $\rho$ , m, E are obtained, derivatives of u and e can be computed by product and quotient rules, e.g.,  $u = \frac{m}{\rho} \Rightarrow u_x = \frac{\rho m_x - m \rho_x}{\rho^2}$ .

#### 4. An alternative positivity-preserving finite difference WENO scheme

In Section 3, we have constructed a WENO scheme solving compressible NS equations by combining the advection flux  $\mathbf{F}^a$  and the diffusion flux  $\mathbf{F}^d$  in the WENO reconstruction. However, in practice one might prefer not to regard  $\mathbf{F}^a - \mathbf{F}^d$  as a single flux. For instance, if a positivity-preserving WENO scheme for compressible Euler equations such as [34] is already available, then one might prefer a positivity-preserving WENO scheme for directly approximating the diffusion flux  $\mathbf{F}^d$ . In this section, we describe such a positivity-preserving WENO scheme based on existing Euler solvers in [34]. The objective of this section is to design a positivity-preserving diffusion flux for  $\mathbf{F}^d$ , rather than regard  $\mathbf{F}^a - \mathbf{F}^d$  as a single flux in the WENO reconstruction.

For simplicity, we only discuss sufficient conditions for positivity in forward Euler time discretization in one dimension. The extension to two dimensions is straightforward since the finite difference scheme is defined in the dimension-by-dimension fashion, as shown in Section 3. Discussion for the positivity-preserving limiter, high order time discretizations and implementation are the same as in Section 3. The same notation in Section 3 will be used.

#### 4.1. One-dimensional scheme

Consider the following finite difference scheme

$$\mathbf{U}_{i}^{n+1} = \mathbf{U}_{i}^{n} - \frac{\Delta t}{\Delta x} (\widehat{\mathbf{F}}_{i+\frac{1}{2}}^{a} - \widehat{\mathbf{F}}_{i-\frac{1}{2}}^{a}) + \frac{\Delta t}{\Delta x} (\widehat{\mathbf{F}}_{i+\frac{1}{2}}^{d} - \widehat{\mathbf{F}}_{i-\frac{1}{2}}^{d}). \tag{4.1}$$

For the advection flux  $\mathbf{F}^a$ , we use the same Lax-Friedrichs flux splitting in [34],

$$\mathbf{Z}^{a,\pm}(\mathbf{U}) = \frac{1}{2}(\mathbf{U} \pm \frac{\mathbf{F}^{a}(\mathbf{U})}{\alpha}) \tag{4.2}$$

with  $\alpha = \max ||(|u|+c)||$ , u and c are the velocity and speed of sound of the state  $\mathbf{U}_i^n$ , the maximum is taken either globally or locally over the  $\mathbf{U}_i^n$  in the WENO reconstruction stencil. For simplicity, we take the maximum globally over the  $\mathbf{U}_i^n$ . For the diffusion flux  $\mathbf{F}^d$ , we use the following local flux splitting. For a (2r+1)-th order WENO scheme, at a fixed index  $i+\frac{1}{2}$ , define

$$(\mathbf{Z}_{i+\frac{1}{2}}^{d,\pm})_{j}^{n} = \frac{1}{2} (\mathbf{U}_{j}^{n} \mp \frac{\mathbf{F}^{d}(\mathbf{U}_{j}^{n}, \mathbf{S}_{j}^{n})}{\beta_{i+\frac{1}{2}}^{d}}), j = i - r, \dots, i + r + 1,$$

$$(4.3)$$

where

$$\beta_{i+\frac{1}{2}}^{d} > \max \left[ \frac{1}{2\rho^{2}e} (\sqrt{\rho^{2}q^{2} + 2\rho^{2}e|\tau|^{2}} + \rho|q|) \right]$$
(4.4)

and the maximum is taken locally over the WENO reconstruction stencil  $\{i-r,\cdots,i+r+1\}$ . Notice that  $\beta^d_{i+\frac{1}{2}}$  here has no specific physical meaning either. The advection flux  $\widehat{\mathbf{F}}^a_{i+\frac{1}{2}}$  can be computed exactly the same as in [34]. We emphasize that signs in (4.3) must be flipped for the correct upwinding bias, i.e.,  $\mathbf{Z}^{d,+} = \frac{1}{2}(\mathbf{U} - \mathbf{F}^d/\beta^d)$  and  $\mathbf{Z}^{d,-} = \frac{1}{2}(\mathbf{U} + \mathbf{F}^d/\beta^d)$ .

At each fixed  $x_{i+\frac{1}{2}}$ , the diffusion flux  $\widehat{\mathbf{F}}_{i+\frac{1}{2}}^d$  is computed as follows.

1. Let  $\mathbf{H}_{i+\frac{1}{2}}^{d,\pm} = R_{\Delta X}(\mathbf{Z}_{i+\frac{1}{2}}^{d,\pm})$ , we can obtain the cell averages at time level n

$$(\overline{\mathbf{H}}_{i+\frac{1}{2}}^{d,\pm})_{j}^{n} = (\mathbf{Z}_{i+\frac{1}{2}}^{d,\pm})_{j}^{n}, \quad j = i - r, \cdots, i + r + 1.$$

2. Transform the cell averages  $(\overline{\mathbf{H}}_{i+\frac{1}{2}}^{d,\pm})_j^n$  from the physical space to the local characteristic space of the Roe matrix by

$$(\overline{\mathbf{T}_{i+\frac{1}{2}}^{\pm}})_{j}^{n} = L_{i+\frac{1}{2}}(\overline{\mathbf{H}_{i+\frac{1}{2}}^{d,\pm}})_{j}^{n}, \quad j = i-r, \cdots, i+r+1.$$

3. Perform the (2r+1)-th order WENO reconstruction for each component of  $(\overline{\mathbf{T}_{i+\frac{1}{2}}^+})_j^n$  to construct nodal values of  $L_{i+\frac{1}{2}}\mathbf{H}_{i+\frac{1}{2}}^{d,+}$  at  $x_{i+\frac{1}{2}}$ , denoted by  $(\mathbf{T}_{i+\frac{1}{2}}^+)_{i+\frac{1}{2}}^{\pm}$ . Perform the (2r+1)-th order WENO reconstruction for each component of  $(\overline{\mathbf{T}_{i+\frac{1}{2}}^-})_j^n$  to construct nodal values of  $L_{i+\frac{1}{2}}\mathbf{H}_{i+\frac{1}{2}}^{d,-}$  at  $x_{i+\frac{1}{2}}$ , denoted by  $(\mathbf{T}_{i+\frac{1}{2}}^-)_{i+\frac{1}{2}}^{\pm}$ .

4. Transform from the local characteristic space back into the physical space by

$$(\mathbf{H}_{i+\frac{1}{2}}^{d,+})_{i+\frac{1}{2}}^{-} = R_{i+\frac{1}{2}}(\mathbf{T}_{i+\frac{1}{2}}^{+})_{i+\frac{1}{2}}^{-}, \quad (\mathbf{H}_{i+\frac{1}{2}}^{d,-})_{i+\frac{1}{2}}^{+} = R_{i+\frac{1}{2}}(\mathbf{T}_{i+\frac{1}{2}}^{-})_{i+\frac{1}{2}}^{+}.$$

5. Obtain the numerical diffusion flux by

$$\widehat{\mathbf{F}}_{i+\frac{1}{2}}^{d} = \beta_{i+\frac{1}{2}}^{d} [(\mathbf{H}_{i+\frac{1}{2}}^{d,-})_{i+\frac{1}{2}}^{+} - (\mathbf{H}_{i+\frac{1}{2}}^{d,+})_{i+\frac{1}{2}}^{-}]. \tag{4.5}$$

4.2. Sufficient conditions for positivity of the diffusion flux

The scheme (4.1) can be written as  $\mathbf{U}_i^{n+1} = \frac{1}{2}\mathbf{U}_i^{n+1,a} + \frac{1}{2}\mathbf{U}_i^{n+1,d}$  with

$$\mathbf{U}_i^{n+1,a} = \mathbf{U}_i^n - 2\frac{\Delta t}{\Delta x}(\widehat{\mathbf{F}}_{i+\frac{1}{2}}^a - \widehat{\mathbf{F}}_{i-\frac{1}{2}}^a), \\ \mathbf{U}_i^{n+1,d} = \mathbf{U}_i^n + 2\frac{\Delta t}{\Delta x}(\widehat{\mathbf{F}}_{i+\frac{1}{2}}^d - \widehat{\mathbf{F}}_{i-\frac{1}{2}}^d).$$

Except the extra scalar factor 2 in front of  $\frac{\Delta t}{\Delta x}$ ,  $\mathbf{U}_i^{n+1,a}$  is the finite difference WENO scheme with forward Euler time stepping for compressible Euler equations, thus its positivity can be discussed exactly the same as in [34]. So it suffices to only discuss sufficient conditions for  $\mathbf{U}_i^{n+1,d} \in G$ .

For a fixed i, we have  $\mathbf{U}_i^n = (\overline{\mathbf{H}_{i+\frac{1}{2}}^{d,+}})_i^n + (\overline{\mathbf{H}_{i+\frac{1}{2}}^{d,-}})_i^n = (\overline{\mathbf{H}_{i-\frac{1}{2}}^{d,+}})_i^n + (\overline{\mathbf{H}_{i-\frac{1}{2}}^{d,-}})_i^n$ . Thus we have

$$\mathbf{U}_{i}^{n+1,d} = \mathbf{U}_{i}^{n} + 2\frac{\Delta t}{\Delta x}(\widehat{\mathbf{F}}_{i+\frac{1}{2}}^{d} - \widehat{\mathbf{F}}_{i-\frac{1}{2}}^{d}) = \mathbf{H}_{1} + \mathbf{H}_{2}$$

with

$$\begin{split} \mathbf{H}_1 &= \frac{1}{2} (\overline{\mathbf{H}_{i+\frac{1}{2}}^{d,+}})_i^n + \frac{1}{2} (\overline{\mathbf{H}_{i+\frac{1}{2}}^{d,-}})_i^n - 2 \frac{\Delta t}{\Delta x} \beta_{i+\frac{1}{2}}^d (\mathbf{H}_{i+\frac{1}{2}}^{d,+})_{i+\frac{1}{2}}^- + 2 \frac{\Delta t}{\Delta x} \beta_{i+\frac{1}{2}}^d (\mathbf{H}_{i+\frac{1}{2}}^{d,-})_{i+\frac{1}{2}}^+, \\ \mathbf{H}_2 &= \frac{1}{2} (\overline{\mathbf{H}_{i-\frac{1}{2}}^{d,+}})_i^n + \frac{1}{2} (\overline{\mathbf{H}_{i-\frac{1}{2}}^{d,-}})_i^n + 2 \frac{\Delta t}{\Delta x} \beta_{i-\frac{1}{2}}^d (\mathbf{H}_{i-\frac{1}{2}}^{d,+})_{i-\frac{1}{2}}^- - 2 \frac{\Delta t}{\Delta x} \beta_{i-\frac{1}{2}}^d (\mathbf{H}_{i-\frac{1}{2}}^{d,-})_{i-\frac{1}{2}}^+. \end{split}$$

Notice that the structure of  $\mathbf{H}_1$  and  $\mathbf{H}_2$  are similar to those in Section 3.3 and thus the sufficient conditions for positivity can be derived following the same lines in Section 3.3. We state the main result as the following theorem.

**Theorem 2.** The (2r+1)-th order accurate finite difference WENO diffusion flux in the scheme (4.1) and (4.5) is positivity-preserving, i.e.,  $\mathbf{U}_i^n \in G \Rightarrow \mathbf{U}_i^{n+1,d} \in G$ , if

under the CFL condition

$$\frac{\Delta t}{\Delta x} \max_{i} \beta_{i+\frac{1}{2}}^{d} \le \frac{1}{4N(N-1)},$$

where  $N = \lceil 2r + 3 \rceil$  and

$$\mathbf{P}_{i}^{+,d*} = \frac{(\overline{\mathbf{H}_{i+\frac{1}{2}}^{d,+}})_{i}^{n} - \widehat{\omega}_{N}(\mathbf{H}_{i+\frac{1}{2}}^{d,+})_{i+\frac{1}{2}}^{-}}{1 - \widehat{\omega}_{N}}, \mathbf{P}_{i}^{-,d*} = \frac{(\overline{\mathbf{H}_{i-\frac{1}{2}}^{d,-}})_{i}^{n} - \widehat{\omega}_{1}(\mathbf{H}_{i-\frac{1}{2}}^{d,-})_{i-\frac{1}{2}}^{+}}{1 - \widehat{\omega}_{1}}.$$

#### 5. Numerical results

We consider some representative numerical examples in one and two dimensions for the positivity-preserving (PP) property of the finite difference (FD) WENO schemes, to demonstrate the performance. We test the positivity-preserving approaches in Section 3 and Section 4 on three different high order WENO schemes. We observe no significant difference for the numerical results between two methods in Section 3 and Section 4, thus for simplicity we only show the results computed by the method of the Section 3.

The classical fifth-order and seven-order FD WENO schemes of Jiang and Shu [15] are referred to as the WENO-JS5 and WENO-JS7 schemes. In the literature, there are many improvements and variants of WENO-JS schemes, and we also test one of the variants, the simple fifth-order FD WENO scheme of Zhu and Qiu [36], referred as the WENO-ZQ5 scheme. The linear weights of the WENO-ZQ5 schemes are set as  $\gamma_1 = 0.98$ ,  $\gamma_1 = 0.01$ ,  $\gamma_1 = 0.01$  in all examples unless otherwise specified.

In these tests, one particular aspect is to validate the robustness. Without the positivity-preserving flux and limiter in this paper, WENO-JS5, WENO-JS7 and WENO-ZQ5 schemes will blow up for all one- and two-dimensional examples in this section. With the additional positivity-preserving limiter, one finds by the numerical test that there don't increase a lot of

**Table 5.1** An accuracy test of the PP FD WENO-JS5, WENO-JS7 and WENO-ZQ5 schemes for one-dimensional compressible Navier-Stokes equations with Re=1000 and final time T=0.1. PP limiter: the average of the Ratio of cells using PP limiter to total cells at each time step.

cells at each time step.								
Mesh	WENO-JS5( $\varepsilon = 10^{-15}$ )			WENO-JS7( $\varepsilon = 10^{-15}$ )				
	L <sup>1</sup> error	order	PP limiter	$L^1$ error	order	PP limite		
10	4.65E-02	_	20.0%	1.94E-01	_	53.3%		
20	1.08E-02	2.11	18.9%	1.10E-01	0.82	25.3%		
40	1.22E-03	3.15	19.3%	1.29E-03	6.41	19.9%		
80	6.19E-05	4.30	7.24%	1.02E-05	6.99	9.28%		
160	1.22E-06	5.66	2.76%	6.11E-08	7.38	3.46%		
320	5.96E-08	4.36	0.91%	6.78E-10	6.50	1.00%		
Mesh	WENO-ZQ5( $\varepsilon = 10^{-15}$			)				
		L <sup>1</sup> error		order		PP limite		
10		5.90E-02		_		13.3%		
20	1.15E-02			2.36		33.3%		
40	1.45E-03			2.99		9.52%		
80	3.75E-05			5.28		4.42%		
160	1.85E-06			4.34		1.82%		
320		4.93E-08		5.23		0.87%		
Mesh	WENO-JS5( $\varepsilon = \Delta x^2$ )			WENO-JS7( $\varepsilon = \Delta x^2$ )				
	L <sup>1</sup> error	order	PP limiter	L <sup>1</sup> error	order	PP limite		
10	4.36E-02	_	33.3%	1.52E-01	_	46.7%		
20	1.05E-02	2.05	26.1%	4.39E-02	1.79	15.6%		
40	9.29E-04	3.50	9.62%	6.89E-04	5.99	22.8%		
80	3.40E-05	4.77	4.81%	5.96E-06	6.85	6.19%		
160	1.03E-06	5.05	3.83%	1.64E-08	8.51	2.53%		
320	2.99E-08	5.10	0.20%	9.96E-11	7.36	0.88%		
Mesh		WENO-Z	$Q5(\varepsilon = \Delta x^2)$					
		L <sup>1</sup> error		order		PP limite		
10		3.42E-02		_		46.7%		
20		1.46E-02		1.23		22.8%		
40		4.75E-04		4.94		8.60%		
	1.49E-05			4.99		4.57%		
80	3.28E-07							
80 160		3.28E-07		5.51		3.15%		

computational cost since there is very few cells using the positivity-preserving limiter in each time step. Another aspect we should focus on is the artificial viscosity. The WENO schemes are high order in the sense that the errors are high order for solving smooth solutions. Near shocks, the error of any scheme on a uniform mesh cannot be high order. However, the high order WENO schemes are still much more advantageous for shock problems in the sense that their numerical artificial viscosity is much lower than first and second order accurate schemes. Inevitably, the positivity-preserving flux splitting and the positivity-preserving limiter in Section 3 induce artificial viscosity, which must be validated through these tests.

For computing nonlinear weight in WENO-JS schemes, the constant  $\varepsilon$  to avoid the denominator being zero can influence the accuracy and can be set as  $\varepsilon = \Delta x^2$  to achieve the optimal convergence order [1]. For many shock problems on fine meshes, simply setting  $\varepsilon = 10^{-15}$  can also reduce artificial viscosity. For all examples except the accuracy test in this paper, the choice between  $\varepsilon = 10^{-15}$  and  $\varepsilon = \Delta x^2$  makes marginal difference for WENO-JS5, WENO-JS7 and WENO-ZQ5 schemes. Thus for simplicity, we only show results using  $\varepsilon = 10^{-15}$ .

The reference solution for the accuracy test was generated by a Fourier collocation spectral method using 1280 points and a  $1280 \times 1280$  mesh respectively. The reference solutions for Examples 5.2, 5.3 and 5.4. were generated by a second order PP FD scheme discussed in the Appendix A of the literature [34] by using a fifth order PP WENO flux for convection term and the second order central difference approximation for diffusion term on a mesh of 6400 grid points.

**Example 5.1.** (An accuracy test) We test the accuracy of positivity-preserving FD WENO-JS5, WENO-JS7 and WENO-ZQ5 schemes for one and two dimensional compressible Navier-Stokes equations with Re = 1000. The initial condition is  $\rho = 1$ , u = 0,  $E = (10^{-10} + \sin^8(x))/(\gamma - 1)$  on the interval  $[0, 2\pi]$  for 1D case;  $\rho = 1$ , u = v = 0,  $E = (10^{-10} + \sin^8(x + y))/(\gamma - 1)$  on the rectangle domain  $[0, 2\pi] \times [0, 2\pi]$  for 2D case. The boundary condition is periodic and final computing time T = 0.1. The minimal value of exact solution energy E is  $2.56 \times 10^{-10}$  for 1D case and  $3.45 \times 10^{-10}$  for 2D case. For comparison, the  $L^1$  errors and numerical order of accuracy by WENO-JS5, WENO-JS7 and WENO-ZQ5 schemes are shown in Table 5.1 and 5.2 to verify the accuracy of the convection diffusion WENO flux and the PP limiter will not destroy the high order accuracy of the schemes. We test the accuracy test with  $E = 10^{-15}$  and  $E = 10^{-15}$ 

**Table 5.2** An accuracy test of the PP FD WENO-JS5, WENO-JS7 and WENO-ZQ5 schemes for two-dimensional compressible Navier-Stokes equations with Re=1000 and final time T=0.1. PP limiter: the average of the Ratio of cells using PP limiter to total cells at each time step.

time step.														
Mesh	WENO-JS5( $\varepsilon = 10^{-15}$ )			WENO-JS7( $\varepsilon = 10^{-15}$ )										
	L <sup>1</sup> error	order	PP limiter	L <sup>1</sup> error	order	PP limiter								
10 × 10	2.17E-01	_	20.2%	1.08E-01	_	26.7%								
$20 \times 20$	1.28E-02	4.08	11.7%	2.10E-02	2.37	24.2%								
$40 \times 40$	1.91E-03	2.75	14.8%	3.70E-03	2.51	10.5%								
$80 \times 80$	1.35E-04	3.83	4.97%	2.05E-05	7.50	5.00%								
$160 \times 160$	3.15E-06	5.42	2.32%	1.16E-07	7.47	2.34%								
$320\times320$	1.07E-07	4.88	0.75%	1.27E-09	6.51	0.37%								
Mesh		WENO-Z	$Q5(\varepsilon = 10^{-15}$	)										
		L <sup>1</sup> error		order		PP limiter								
10 × 10		2.73E-01		_		3.33%								
$20 \times 20$		2.03E-02		3.75		9.00%								
$40 \times 40$	$40 \times 40$		3.02E-03			9.57%								
$80 \times 80$	< 80		5.18E-05			2.48%								
$160 \times 160$	$160 \times 160$		5.87E-06			0.86%								
$320\times320$		2.14E-07		4.78		0.60%								
Mesh	WENO-JS5( $\varepsilon = \Delta x^2$ )			WENO-JS7( $\varepsilon = \Delta x^2$ )										
	L <sup>1</sup> error	order	PP limiter	L <sup>1</sup> error	order	PP limiter								
10 × 10	2.17E-01	_	30.7%	1.07E-01	_	33.3%								
$20 \times 20$	4.22E-02	2.37	16.7%	2.35E-02	2.18	20.8%								
$40 \times 40$	2.43E-03	4.12	9.10%	3.67E-03	2.68	7.69%								
$80 \times 80$	6.75E-05	5.17	4.91%	9.73E-06	8.56	2.88%								
$160 \times 160$	2.15E-06	4.97	1.22%	4.10E-08	7.89	2.50%								
320 × 320	6.20E-08	5.12	0.01%	2.32E-10	7.47	0.31%								
						WENO-ZQ5( $\varepsilon = \Delta x^2$ )								
Mesh		WENO-Z	$Q5(\varepsilon = \Delta x^2)$											
Mesh		WENO-Z	$Q5(\varepsilon = \Delta x^2)$	order		PP limiter								
Mesh 10 × 10			$Q5(\varepsilon = \Delta x^2)$	order –		PP limiter 56.7%								
		L <sup>1</sup> error		order - 2.53										
10 × 10		L <sup>1</sup> error 1.42E-01		_		56.7%								
10 × 10 20 × 20		L <sup>1</sup> error 1.42E-01 2.46E-02		_ 2.53		56.7% 18.7%								
10 × 10 20 × 20 40 × 40		L <sup>1</sup> error 1.42E-01 2.46E-02 1.78E-03		_ 2.53 3.79		56.7% 18.7% 10.3%								
$   \begin{array}{c}     10 \times 10 \\     20 \times 20 \\     40 \times 40 \\     80 \times 80   \end{array} $		1.42E-01 2.46E-02 1.78E-03 3.47E-05		- 2.53 3.79 5.68		56.7% 18.7% 10.3% 2.48%								

the fifth-order accuracy with  $\varepsilon=10^{-15}$  and  $\Delta x^2$ . WENO-JS7 has smaller  $L_1$  errors than WENO-JS5 and WENO-ZQ5, suffering certain order loss with  $\varepsilon=10^{-15}$  but achieving optimal seven-order accuracy with  $\varepsilon=\Delta x^2$ . For the accuracy test, the time step  $\Delta t$  is set as  $\Delta t=\min\{0.6\Delta x^{\frac{5}{3}},0.001\text{Re}\Delta x^2\}$  for WENO-JS5 and WENO-ZQ5, and  $\Delta t=\min\{0.6\Delta x^{\frac{7}{3}},0.001\text{Re}\Delta x^2\}$  for WENO-JS7.

**Example 5.2.** (Double rarefaction problem) This problem [17] has the low pressure and low density regions. The initial condition is  $(\rho, u, p, \gamma) = (7, -1, 0.2, 1.4)$  for  $x \in [-1, 0)$  and  $(\rho, u, p, \gamma) = (7, 1, 0.2, 1.4)$  for  $x \in [0, 1]$ . The final computing time is T = 0.6. The left and right boundary conditions are inflow and outflow respectively. The numerical results of PP FD WENO-JS5, WENO-JS7 and WENO-ZQ5 schemes for Re = 1000 are shown in Fig. 5.1, which are comparable to the results of PP DG method in [28]. From the density zoomed (right) in the Fig. 5.1, we can see that the PP FD WENO-ZQ5 scheme has better performance than PP FD WENO-JS5 and PP FD WENO-JS7 schemes.

**Example 5.3.** (1D Sedov blast wave problem) The Sedov blast wave problem contains both very low density and strong shocks and is difficult to be simulated precisely. The exact solution is specified in [16,23]. The computational domain is [-2,2] and initial conditions are that the density is 1, the velocity is 0, the total energy is  $10^{-12}$  everywhere except in the center cell, which is a constant  $E_0/\Delta x$  with  $E_0 = 3200000$ , with  $\gamma = 1.4$ . The final computing time is T = 0.001. The inlet and outlet conditions are imposed on the left and right boundaries, respectively. The computational results of PP FD WENO-JS5, WENO-JS7 and WENO-ZQ5 schemes for R = 1000 are shown in Fig. 5.2. We can see that PP FD WENO-JS5, WENO-JS7 and WENO-ZQ5 schemes work well for this extreme 1D test case.

**Example 5.4.** (Leblanc problem) The initial condition of Leblanc problem [17] is  $(\rho, u, p, \gamma) = (2, 0, 10^9, 1.4)$  for  $x \in [-10, 0)$  and  $(\rho, u, p, \gamma) = (0.001, 0, 1, 1.4)$  for  $x \in [0, 10]$ . The left and right boundary conditions are also inflow and outflow respectively, and the computing time is T = 0.001. See the Fig. 5.3 for results of PP FD WENO-JS5, WENO-JS7 and WENO-ZQ5

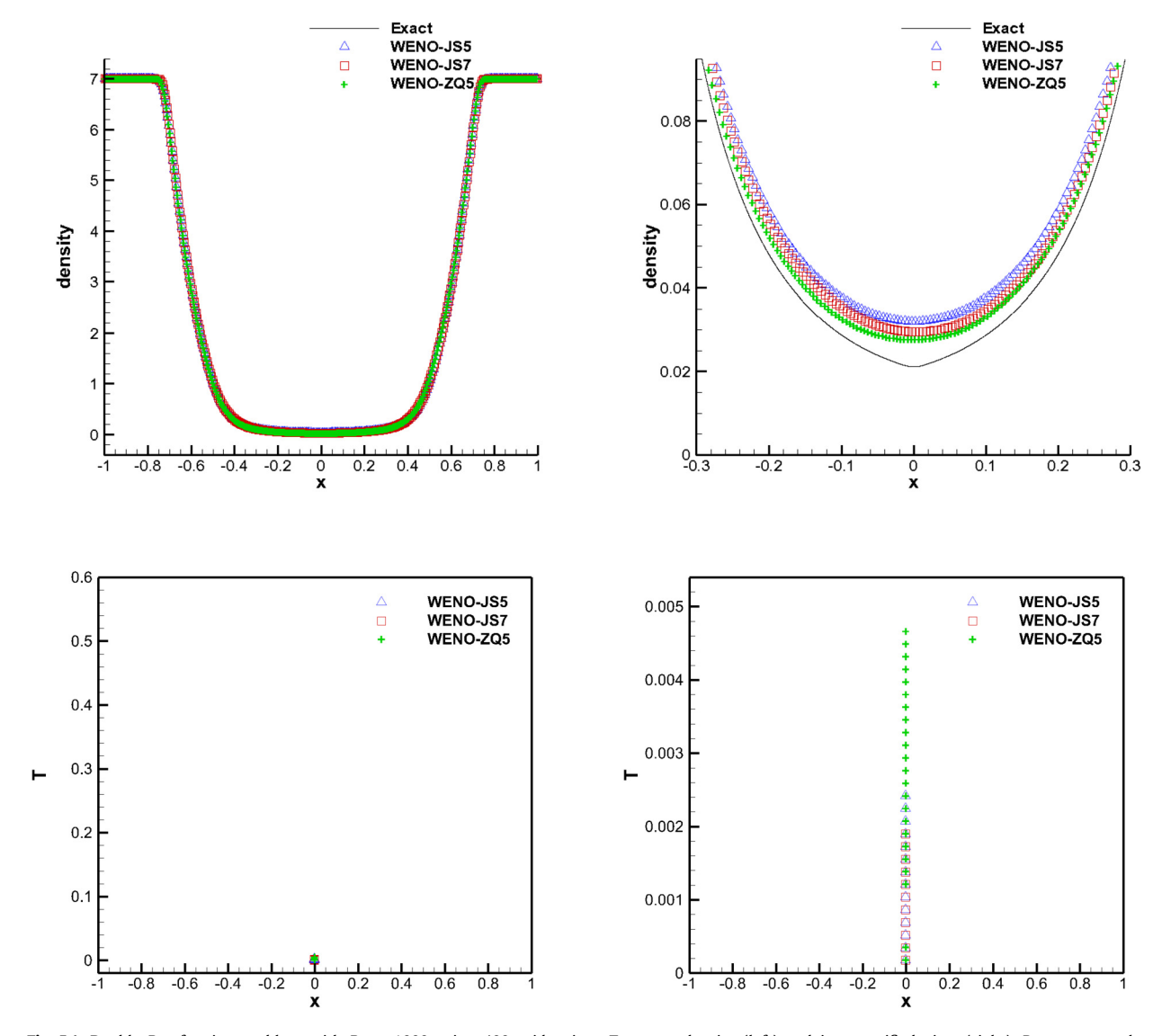


Fig. 5.1. Double Rarefraction problem with Re = 1000 using 400 grid points. Top row: density (left) and its magnified view (right). Bottom row: the space-time location where the PP limiter is triggered (left) and its magnified view (right).

schemes for Re = 1000 shown in Fig. 5.3. The PP FD WENO-ZQ5 scheme produces more oscillation possibly due to its wider stencil in reconstruction.

**Example 5.5.** (2D Sedov blast wave problem) The computational domain is a square of  $[0, 1.1] \times [0, 1.1]$ . For the initial condition, similar to the 1D case, the density is 1, the velocity is 0, the total energy is  $10^{-12}$  everywhere except in the lower left corner is the constant  $\frac{0.244816}{\Delta x \Delta y}$  and  $\gamma = 1.4$  in the ideal gas EOS. The numerical boundary conditions on the left and bottom edges are reflective. The numerical boundary conditions on the right and top are outflow. The final time is T=1. For comparison, we present the numerical results of density for Re = 1000 and  $\infty$  in Fig. 5.4 by the PP FD WENO-JS5, WENO-JS7 and WENO-ZQ5 schemes. The average of the Ratio of cells using PP limiter to total cells at each time step is 0.303%, 0.248%, 0.299% in Re= $\infty$  and 0.309%, 0.119%, 0.139% in Re=1000 for the PP FD WENO-JS5, WENO-JS7 and WENO-ZQ5 schemes respectively. The numerical results demonstrate the good performance of the PP FD WENO-JS5, WENO-JS7 and WENO-ZQ5 schemes.

**Example 5.6.** (Shock diffraction problem) Shock passing a backward facing corner (diffraction) has been used as a positivity test problem for the DG method in [3]. It is easy to get negative density and/or pressure below and to the right of the corner. The computational domain is the union of  $[0,1] \times [6,11]$  and  $[1,13] \times [0,11]$ . The initial condition is a pure rightmoving shock of Mach number 5.09, initially located at x = 0.5 and  $6 \le y \le 11$ , moving into undisturbed air ahead of the shock with a density of 1.4 and a pressure of 1. The boundary conditions are inflow at x = 0,  $6 \le y \le 11$ , outflow at x = 0.

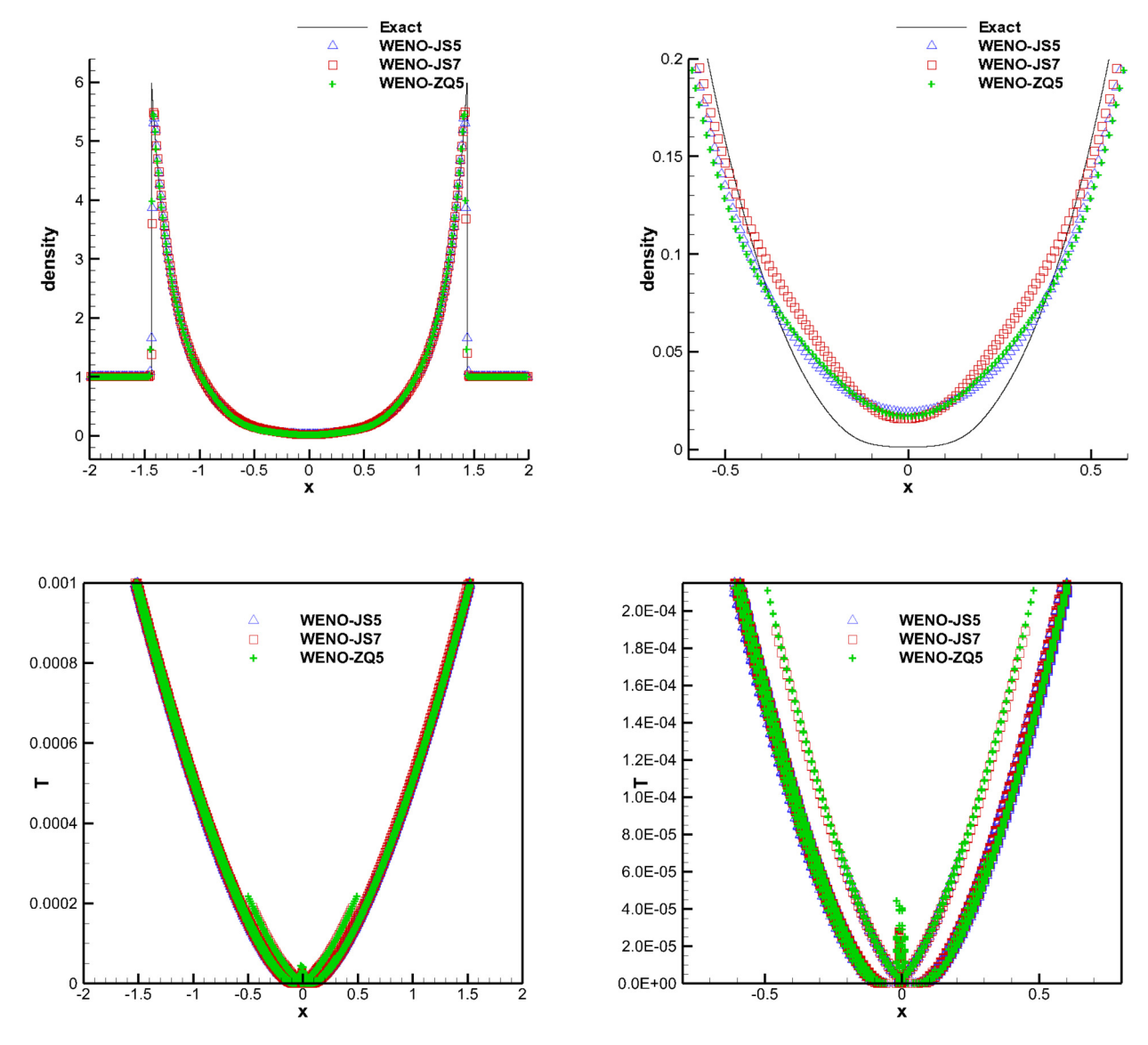
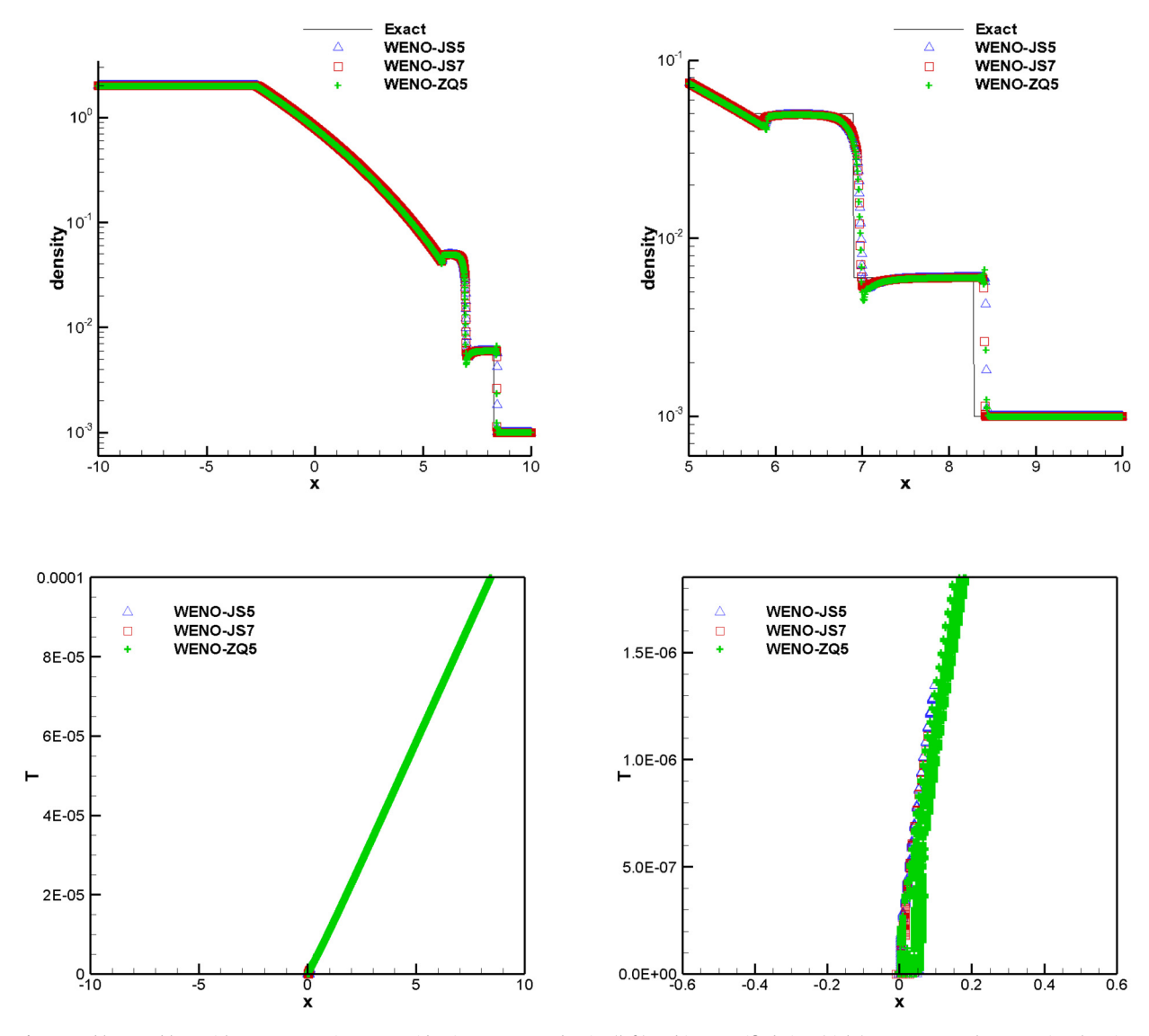


Fig. 5.2. Sedov1D problem with Re = 1000 using 400 grid points. Top row: density (left) and its magnified view (right). Bottom row: the space-time location where the PP limiter is triggered (left) and its magnified view (right).

 $13, 0 \le y \le 11, 1 \le x \le 13, y = 0$  and  $0 \le x \le 13, y = 11$ , and reflective at the walls  $0 \le x \le 1, y = 6$  and at  $x = 1, 0 \le y \le 6$ . The average of the Ratio of cells using PP limiter to total cells at each time step is 0.0024%, 0.0026%, 0.0125% in Re= $\infty$  and 0.0005%, 0.0010%, 0.0079% in Re=1000 for the PP FD WENO-JS5, WENO-JS7 and WENO-ZQ5 schemes respectively. The numerical results of density for Re= 1000 and  $\infty$  at final time T = 2.3 by the PP FD WENO-JS5, WENO-JS7 and WENO-ZQ5 schemes are presented in Fig. 5.5.

**Example 5.7.** (Mach 2000 astrophysical jet problem) For simulating the gas dynamical jets and shocks imaged by the Hubble Space Telescope, one can implement theoretical models in a gas dynamics simulator [7,12,13]. We consider the Mach 2000 astrophysical jets without the radiative cooling to demonstrate the robustness of our method. The computational domain is  $[0,1] \times [-0.25,0.25]$  and initially full of the ambient gas with  $(\rho,u,v,p,\gamma)=(0.5,0,0,0.4127,5/3)^T$ . The boundary conditions for the right, top, and bottom are outflow. For the left boundary  $(\rho,u,v,p,\gamma)=(0.5,800,0,0.4127,5/3)^T$  for  $y \in [-0.05,0.05]$  and  $(\rho,u,v,p,\gamma)=(0.5,0,0,0.4127,5/3)^T$  otherwise. The terminal time is T=0.001. The simulation results of density for Re= 1000 and  $\infty$  by the PP FD WENO-JS5, WENO-JS7 and WENO-ZQ5 schemes are shown in Fig. 5.6. The average of the Ratio of cells using PP limiter to total cells at each time step is 0.178%, 0.230%, 0.416% in Re= $\infty$  and 0.103%, 0.070%, 0.225% in Re=1000 for the PP FD WENO-JS5, WENO-JS7 and WENO-ZQ5 schemes respectively. One can see these schemes work well for this test with advantages that negative density and pressure never appear. We emphasize that WENO schemes without any positivity treatment will simply blow up for this test.



**Fig. 5.3.** Leblanc problem with Re = 1000 using 3200 grid points. Top row: density (left) and its magnified view (right). Bottom row: the space-time location where the PP limiter is triggered (left) and its magnified view (right).

**Example 5.8.** (Mach 10 shock reflection and diffraction problem) The computational domain is the union of  $[0,1] \times [0,1]$ and  $[-1,1] \times [1,3]$ . The initial condition is a pure right-moving Mach 10 shock located at  $x=\frac{1}{6}$ , y=0, making a 60° angle with the x-axis. The boundary conditions are set up as follows: reflective boundary condition is used at the wall  $\frac{1}{6} \le x \le 1$ , y = 0 and  $x = 1, -1 \le y \le 0$ ; for the boundary from x = 0 to  $x = \frac{1}{6}$  and y = 0, the exact post-shock condition is posed; the top boundary is the exact motion of mach 10 shock and  $\gamma = 1.4$  for compressible Euler equations; inflow boundary condition is used for the left edges; outflow boundary condition is applied at right and bottom edges. This test case is a combination of reflection and diffraction of shock involving not only shock but also low density, low pressure and complicated fine structure due to the Kelvin-Helmholtz instability generated in the reflection. The reflection part is exactly the same as the benchmark test referred as double mach reflection. We present the simulation result of density at final time T = 0.2 for Re = 1000 and  $\infty$  by the PP FD WENO-JS5, WENO-JS7 and WENO-ZQ5 schemes in Fig. 5.7 to verify the robustness and efficiency of the proposed PP FD schemes. The average of the Ratio of cells using PP limiter to total cells at each time step is 0.0017%, 0.0016%, 0.0034% in Re= $\infty$  and 0.0002%, 0.0001%, 0.0009% in Re=1000 for the PP FD WENO-JS5, WENO-JS7 and WENO-ZQ5 schemes respectively. Compared with the result of Re  $=\infty$ , we can see that the result of Re = 1000 smears the fine feature generated by the Kelvin-Helmholtz instability due to numerical viscosity and extra physical viscosity of compressible NS equations. On the other hand, the numerical results demonstrate that positivity flux and limiter does not induce excessive numerical viscosity in WENO schemes, which still can capture fine feature generated by the Kelvin-Helmholtz instability. In particular, the PP FD WENO-ZQ5 performs better than PP FD WENO-JS5, WENO-JS7, with lower artificial viscosity.

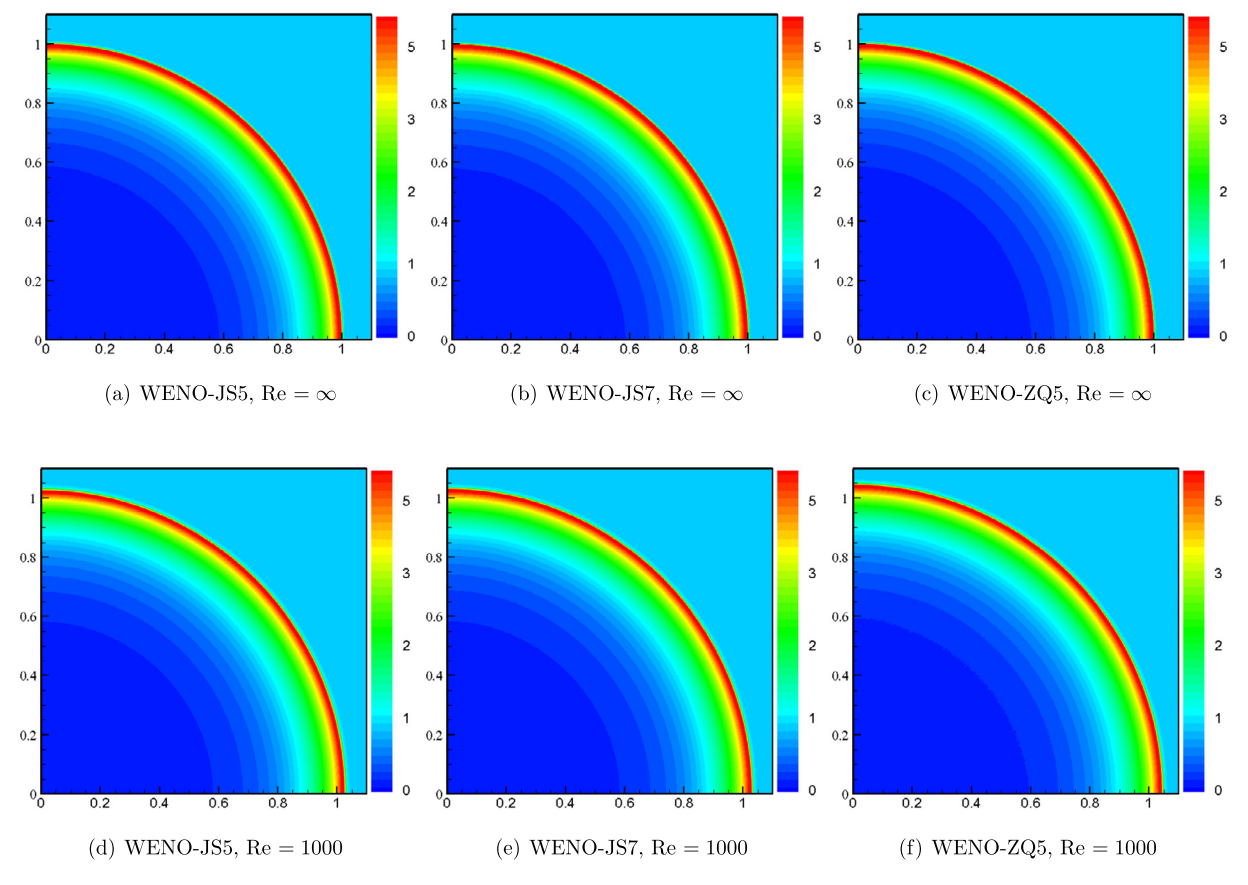


**Fig. 5.4.** 2D Sedov blast wave problem. 20 equally spaced density contour lines from 0.1 to 5. Mesh size:  $\Delta x = \Delta y = \frac{1.1}{320}$ .

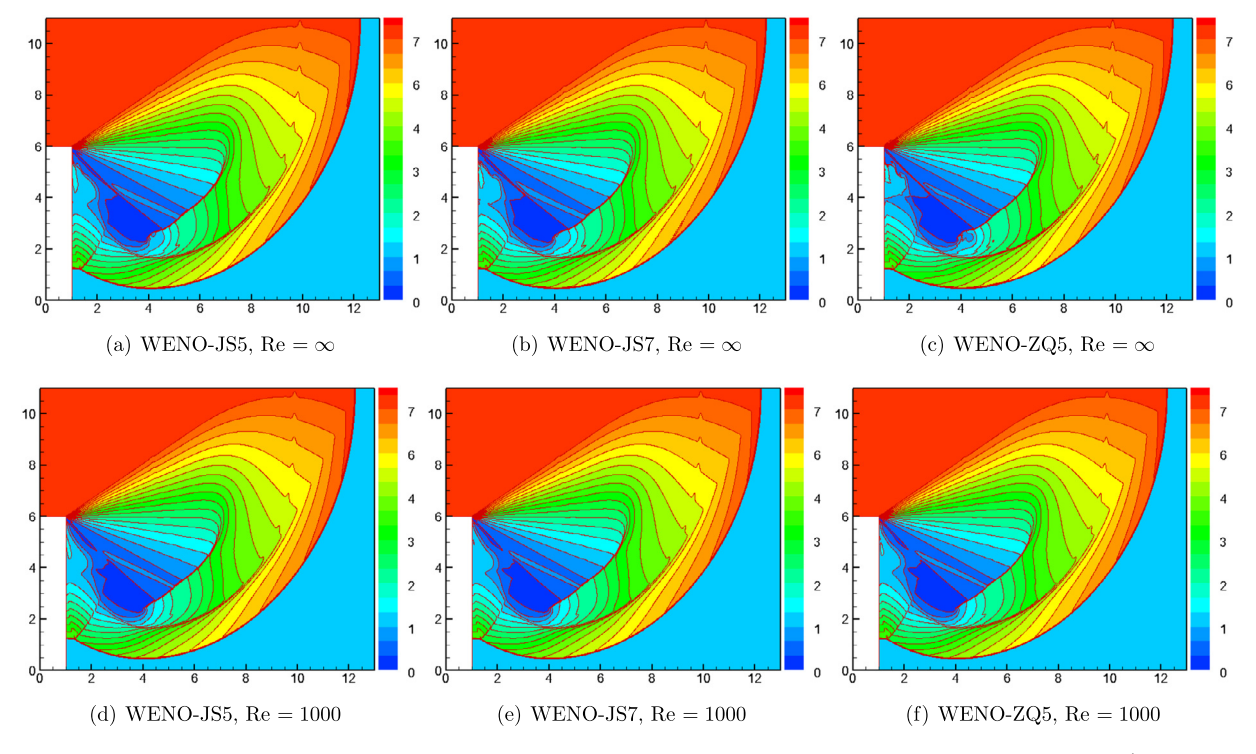


**Fig. 5.5.** Shock diffraction problem. 20 equally spaced density contour lines from 0.066227 to 7.0668. Mesh size:  $\Delta x = \Delta y = \frac{1}{64}$ .

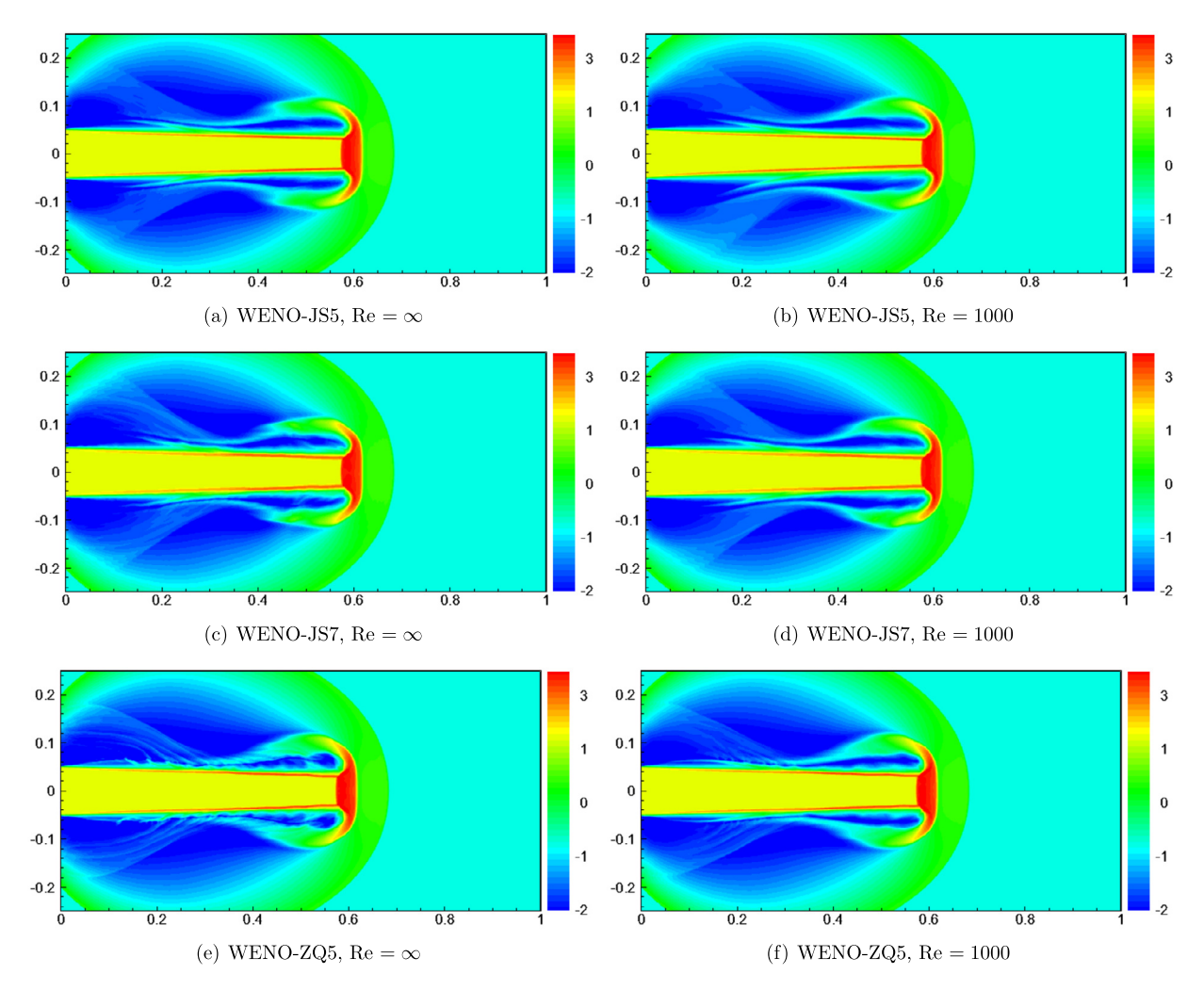


**Fig. 5.6.** Simulation of Mach 2000 jet without radiative cooling problem. Scales are logarithmic. 40 equally spaced density contours from -2 to 3. Mesh size:  $\Delta x = \Delta y = \frac{1}{640}$ .

#### 6. Concluding remarks

We propose an approach of constructing positivity-preserving finite difference WENO schemes for compressible Navier-Stokes equations by using a positivity-preserving convection diffusion flux splitting and a positivity-preserving limiter in the WENO reconstruction. The new flux splitting is quite different from a conventional WENO method for a convection diffusion problem, numerical results on demanding problems for PP FD WENO-JS5, WENO-JS7 and WENO-ZQ5 schemes demonstrate that its performance is quite satisfying thanks to much improved robustness. Moreover, the positivity-preserving approach does not induce excessive artificial viscosity in these high order WENO schemes.

#### **CRediT authorship contribution statement**

**Chuan Fan:** Methodology, Software, Writing – original draft. **Xiangxiong Zhang:** Conceptualization, Methodology, Writing – review & editing. **Jianxian Qiu:** Conceptualization, Methodology, Supervision, Writing – review & editing.

#### **Declaration of competing interest**

The authors declare the following financial interests/personal relationships which may be considered as potential competing interests:

Jianxian Qiu reports financial support was provided by National Natural Science Foundation of China. Xiangxiong Zhang reports financial support was provided by National Science Foundation.

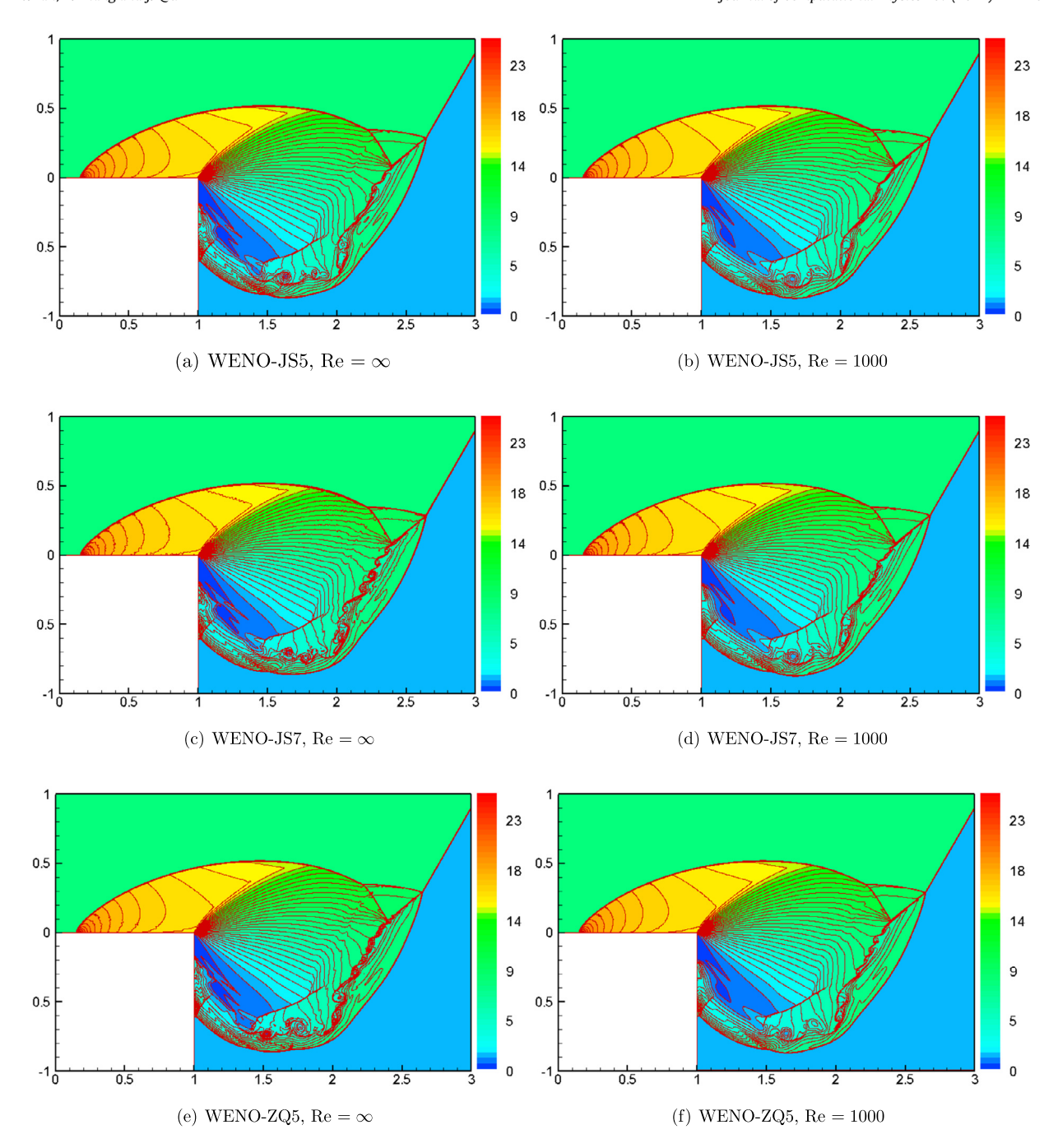


**Fig. 5.7.** Simulation of Mach 10 shock reflection and diffraction problem. 50 equally spaced density contours from 0 to 25. Mesh size:  $\Delta x = \Delta y = \frac{1}{480}$ .

#### References

- [1] F. Aràndiga, A. Baeza, A. Belda, P. Mulet, Analysis of WENO schemes for full and global accuracy, SIAM J. Numer. Anal. 49 (2011) 893-915.
- [2] P. Batten, N. Clarke, C. Lambert, D.M. Causon, On the choice of wavespeeds for the HLLC Riemann solver, SIAM J. Sci. Comput. 18 (1997) 1553-1570.
- [3] B. Cockburn, C.-W. Shu, The Runge–Kutta discontinuous Galerkin method for conservation laws V: multidimensional systems, J. Comput. Phys. 141 (1998) 199–224.
- [4] B. Einfeldt, C.-D. Munz, P.L. Roe, B. Sjögreen, On Godunov-type methods near low densities, J. Comput. Phys. 92 (1991) 273–295.
- [5] C. Fan, X. Zhang, J. Qiu, Positivity-preserving high order finite volume hybrid Hermite WENO scheme for compressible Navier-Stokes equations, J. Comput. Phys. 445 (2021) 110596.
- [6] R.P. Fedkiw, T. Aslam, B. Merriman, S. Osher, A non-oscillatory Eulerian approach to interfaces in multimaterial flows (the ghost fluid method), J. Comput. Phys. 152 (1999) 457–492.
- [7] C.L. Gardner, S.J. Dwyer, Numerical simulation of the xz tauri supersonic astrophysical jet, Acta Math. Sci. 29 (2009) 1677-1683.

- [8] D. Grapsas, R. Herbin, W. Kheriji, J.-C. Latché, An unconditionally stable staggered pressure correction scheme for the compressible Navier-Stokes equations, SMAI J. Comput. Math. 2 (2016) 51–97.
- [9] J. Gressier, P. Villedieu, J.-M. Moschetta, Positivity of flux vector splitting schemes, J. Comput. Phys. 155 (1999) 199-220.
- [10] J.-L. Guermond, M. Maier, B. Popov, I. Tomas, Second-order invariant domain preserving approximation of the compressible Navier-Stokes equations, Comput. Methods Appl. Mech. Eng. 375 (2021) 113608.
- [11] Y. Guo, T. Xiong, Y. Shi, A positivity-preserving high order finite volume compact-WENO scheme for compressible Euler equations, J. Comput. Phys. 274 (2014) 505–523.
- [12] Y. Ha, C.L. Gardner, Positive scheme numerical simulation of high Mach number astrophysical jets, J. Sci. Comput. 34 (2008) 247-259.
- [13] Y. Ha, C.L. Gardner, A. Gelb, C.-W. Shu, Numerical simulation of high Mach number astrophysical jets with radiative cooling, J. Sci. Comput. 24 (2005) 29–44.
- [14] X.Y. Hu, N. Adams, C.-W. Shu, Positivity-preserving method for high-order conservative schemes solving compressible Euler equations, J. Comput. Phys. 242 (2013) 169–180.
- [15] G.-S. Jiang, C.-W. Shu, Efficient implementation of weighted ENO schemes, J. Comput. Phys. 126 (1996) 202-228.
- [16] V.P. Korobeinikov, Problems of Point Blast Theory, American Institute of Physics, College Park, 1991.
- [17] T. Linde, P. Roe, Robust Euler codes, AIAA paper-97-2098, in: 13th Computational Fluid Dynamics Conference, Snowmass Village, CO, 1997.
- [18] X.-D. Liu, S. Osher, T. Chan, Weighted essentially non-oscillatory schemes, J. Comput. Phys. 115 (1994) 200-212.
- [19] Y. Liu, C.-W. Shu, M. Zhang, High order finite difference WENO schemes for nonlinear degenerate parabolic equations, SIAM J. Sci. Comput. 33 (2011) 939–965.
- [20] Y. Liu, C.-w. Shu, M.-p. Zhang, On the positivity of linear weights in WENO approximations, Acta Math. Appl. Sin. Engl. Ser. 25 (2009) 503-538.
- [21] B. Perthame, C.W. Shu, On positivity preserving finite volume schemes for Euler equations, Numer. Math. 73 (1996) 119-130.
- [22] D.C. Seal, Q. Tang, Z. Xu, A.J. Christlieb, An explicit high-order single-stage single-step positivity-preserving finite difference WENO method for the compressible Euler equations, J. Sci. Comput. (2016).
- [23] L.I. Sedov, Similarity and Dimensional Methods in Mechanics, Academic Press, New York, 1959.
- [24] J. Shi, C. Hu, C.-W. Shu, A technique of treating negative weights in WENO schemes, J. Comput. Phys. 175 (2002) 108-127.
- [25] C.-W. Shu, Essentially non-oscillatory and weighted essentially non-oscillatory schemes, Acta Numer, 29 (2020) 701-762.
- [26] T. Tang, K. Xu, Gas-kinetic schemes for the compressible Euler equations: positivity-preserving analysis, Z. Angew. Math. Phys. ZAMP 50 (1999) 258-281.
- [27] T. Xiong, J.-M. Qiu, Z. Xu, Parametrized positivity preserving flux limiters for the high order finite difference WENO scheme solving compressible Euler equations, J. Sci. Comput. 67 (2016) 1066–1088.
- [28] X. Zhang, On positivity-preserving high order discontinuous Galerkin schemes for compressible Navier-Stokes equations, J. Comput. Phys. 328 (2017) 301–343.
- [29] X. Zhang, Y. Liu, C.-W. Shu, Maximum-principle-satisfying high order finite volume weighted essentially nonoscillatory schemes for convection-diffusion equations, SIAM J. Sci. Comput. 34 (2012) A627–A658.
- [30] X. Zhang, C.-W. Shu, On maximum-principle-satisfying high order schemes for scalar conservation laws, J. Comput. Phys. 229 (2010) 3091–3120.
- [31] X. Zhang, C.-W. Shu, On positivity-preserving high order discontinuous Galerkin schemes for compressible Euler equations on rectangular meshes, J. Comput. Phys. 229 (2010) 8918–8934.
- [32] X. Zhang, C.-W. Shu, Maximum-principle-satisfying and positivity-preserving high-order schemes for conservation laws: survey and new developments, Proc. R. Soc. A, Math. Phys. Eng. Sci. 467 (2011) 2752–2776.
- [33] X. Zhang, C.-W. Shu, Positivity-preserving high order discontinuous Galerkin schemes for compressible Euler equations with source terms, J. Comput. Phys. 230 (2011) 1238–1248.
- [34] X. Zhang, C.-W. Shu, Positivity-preserving high order finite difference WENO schemes for compressible Euler equations, J. Comput. Phys. 231 (2012) 2245–2258.
- [35] X. Zhang, Y. Xia, C.-W. Shu, Maximum-principle-satisfying and positivity-preserving high order discontinuous Galerkin schemes for conservation laws on triangular meshes, J. Sci. Comput. 50 (2012) 29–62.
- [36] J. Zhu, J. Oiu, A new fifth order finite difference WENO scheme for solving hyperbolic conservation laws, J. Comput. Phys. 318 (2016) 110–121.